View metadata, citation and similar papers at core.ac.uk

brought to you by CORE

provided by Digital Repository UL FGG

Univerza
v Ljubljani
Fakulteta
za gradbeništvo
in geodezijo

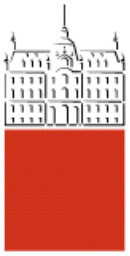

Jamova 2
1000 Ljubljana, Slovenija
http://www3.fgg.uni-lj.si/

DRUGG – Digitalni repozitorij UL FGG
http://drugg.fgg.uni-lj.si/

Ta članek je avtorjeva zadnja recenzirana različica, kot je bila sprejeta po opravljeni recenziji.

Prosimo, da se pri navajanju sklicujte na bibliografske podatke, kot je navedeno:

University
of Ljubljana
Faculty of
Civil and Geodetic
Engineering

Jamova 2
SI – 1000 Ljubljana, Slovenia
http://www3.fgg.uni-lj.si/

DRUGG – The Digital Repository
http://drugg.fgg.uni-lj.si/

This version of the article is author's manuscript as accepted for publishing after the review process.

When citing, please refer to the publisher's bibliographic information as follows:

Brank, B., Mamouri, S., Ibrahimbegović, A. 2005. Constrained finite rotations in dynamic of shells and Newmark implicit time-stepping schemes. *Eng. comput.*, 22, 5-6: 505-535.

DOI: 10.1108/02644400510602998

Constrained Finite Rotations in Dynamics of Shells and Newmark Implicit Time-Stepping Schemes

Boštjan Brank
University of Ljubljana, Faculty of Civil and Geodetic Engineering
Jamova 2, 1000 Ljubljana, Slovenia
Phone +386.1.476.85.94, Fax +386.1.425.06.93
e-mail: bbrank ikpir.fgg.uni-lj.si

Said Mamouri
Université de Technologie de Compiègne U.T.C., Dept. GSM
bp-529 60205 Compiègne, France
e-mail: Said.Mamouri utc.fr

Adnan Ibrahimbegović
Ecole Normale Supérieure de Cachan/LMT
61, av. du président Wilson, 94235 Cachan cedex, France
e-mail: Adnan.Ibrahimbegovic lmt.ens-cachan.fr

October 18, 2004

Abstract

In this work we develop the corresponding version of the Newmark time-stepping schemes for the dynamics of smooth shells employing constrained finite rotations. Different possibilities to choose the constrained rotation parameters are discussed, with the special attention given to our preferred choice of the incremental rotation vector. The pertinent details of consistent linearization, rotation updates and illustrative numerical simulations are supplied.

Key words: shell dynamics, finite rotations, incremental rotation vector, Newmark schemes

1 Introduction

In this work we address the issues pertaining to dynamics of constrained finite rotations as a follow-up from the previous considerations in statics [Ibrahimbegović, Brank and Courtois (2001)]. The present considerations are of direct interest for nonlinear dynamics of smooth shells where, according to the classical shell theory (e.g. see [Naghdi (1972)]), one can eliminate the rotation component around the shell-director and retain only two rotation parameters. Rotations in classical shell models are therefore unrestricted in size but constrained in the space in the direction of the shell-director. There exists a number of possibilities as a choice for the rotation parameters of this kind (e.g. see [Büchter and Ramm (1992), Betsch, Menzel and Stein (1998) or Brank and Ibrahimbegović (2001)] and related works). Among them, we believe, the prominent role is played by the incremental rotation vector [Ibrahimbegović (1997a)] as the most suitable parameter for the standard incremental solution strategy as well as for the construction of the

time-stepping schemes. The latter is examined in more detail in this work in the context of Newmark implicit time-stepping schemes. A number of illustrative examples show a very satisfying performance of the proposed schemes. For the discretization in space a four-noded isoparametric shell finite element with continuum-consistent interpolations is used. This kind of interpolations allow one to treat shell finite rotations exclusively at the element nodes.

The outline of the paper is as follows. In section 2 we recall governing equations for the dynamics of stress resultant geometrically exact shells. Equations are given in terms of the shell-director vector and no particular rotation parameters are yet associated with its rotation. In section 3 we discuss different possibilities which can be chosen for the constrained rotation parameters, and relate those parameters with the shell-director. We focus on the vector-like rotation parameters associated with the rotation vector and on iterative rotation parameters associated with the exponential mapping formula. In section 4 we introduce constrained incremental rotation vector, which is further examined in more detail in section 5 where we develop implicit Newmark time integration schemes for classical smooth shells with constrained rotations. The consistent linearization aspects are addressed in section 6 and some linearized matrices are provided in Appendix. Three numerical examples are presented in section 7.

2 Geometrically exact shell model; dynamic formulation

2.1 Basic kinematic relations

In this work we consider a shell as a single director Cosserat surface (see e.g. [Naghdi (1972), Simo and Fox (1989) or Ibrahimbegović (1997)]). This is a two-dimensional surface (typically chosen as the shell mid-surface) with a so-called director vector attributed to each point of the surface. The position vector for a particular point in a shell deformed configuration is assumed to be defined by the following expression

$$\boldsymbol{\varphi}\left(\xi^1,\xi^2,t\right)+\zeta\mathbf{t}\left(\xi^1,\xi^2,t\right);\left(\xi^1,\xi^2\right)\in\mathcal{A};\zeta\in\mathcal{F}:=\left\{h^-,h^+\right\} \tag{1}$$

where $\mathcal{A}$ defines the domain of the mid-surface parametrization and h^+-h^- is the thickness of the shell. In (1) above, ξ^1 and ξ^2 are convected curvilinear coordinates and ζ is trough the thickness coordinate. Parameter t defines time with the interval of interest defined as $t\in[t_0=0,T]$. It is assumed that the director vector $\mathbf{t}$ remains a unit vector in any deformed configuration, i.e.

$$\|\mathbf{t}\|=1 \tag{2}$$

It follows from (1) that all deformed configurations of the shell are completely determined by pairs $(\boldsymbol{\varphi},\mathbf{t})$. In other words, the configuration space, denoted by $\mathcal{C}$, is then defined by

$$\mathcal{C}:=\left\{(\boldsymbol{\varphi},\mathbf{t}):\mathcal{A}\rightarrow\mathbb{R}^3\times S^2\mid\boldsymbol{\varphi}_{|\partial\mathcal{A}_{\boldsymbol{\varphi}}}=\bar{\boldsymbol{\varphi}},\mathbf{t}_{|\partial\mathcal{A}_{\mathbf{t}}}=\bar{\mathbf{t}}\right\} \tag{3}$$

where S^2 is a unit sphere (a space of all vectors of unit length), while $\partial\mathcal{A}_{\boldsymbol{\varphi}}$ and $\partial\mathcal{A}_{\mathbf{t}}$ are parts of the boundary where the displacement and the director field are specified, respectively.

At each point of the mid-surface in the deformed configuration (at time $t>t_0$) we define the convected frame as

$$\{\mathbf{t}_1,\mathbf{t}_2,\mathbf{t}_3\}:=\left\{\boldsymbol{\varphi}_{,1},\boldsymbol{\varphi}_{,2},\mathbf{t}\right\} \tag{4}$$

where $(\circ)_{,\alpha}\equiv\frac{\partial}{\partial\xi^\alpha}(\circ)$. It is considered that the vector basis in (4) is obtained by mapping of the frame constructed in the shell reference configuration at time $t=t_0$

$$\{\mathbf{g}_1,\mathbf{g}_2,\mathbf{g}_3\}:=\left\{\boldsymbol{\varphi}_{0,1},\boldsymbol{\varphi}_{0,2},\mathbf{t}_0\right\} \tag{5}$$

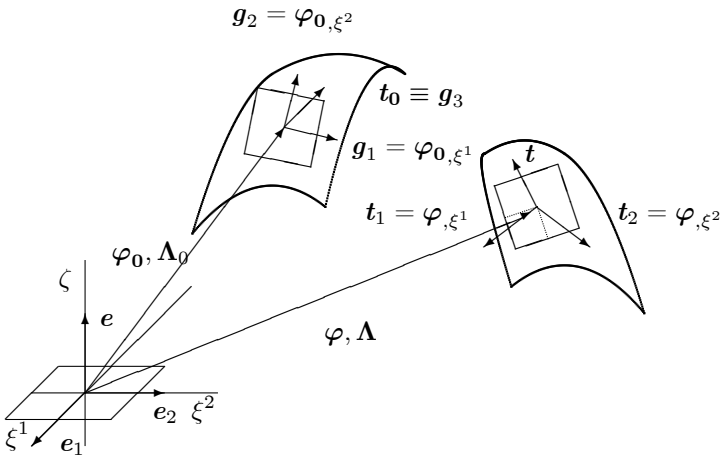

Figure 1: Base vectors in reference and current configuration

where $(\varphi_0, \mathbf{t}_0) \in \mathcal{C}_0$ define the initial positions of the mid-surface and the director field, respectively. Without loss of generality we choose the set of normal coordinates by assuming that the director vector is initially orthogonal to the shell mid-surface, i.e.

$$(\mathbf{g}_1 \times \mathbf{g}_2) \times \mathbf{g}_3 = \mathbf{0} \tag{6}$$

The above concepts are illustrated in Figure 1.

REMARK1. The shell model, completely equivalent to the Cosserat surface model, can be derived from the 3d continuum by employing standard assumptions on the distribution of the displacement field in the shell body and by approximating the terms describing the shell geometry; see e.g. [Büchter and Ramm (1992), Başar and Ding (1990), Brank, Perić and Damjanić (1997), Brank, Briseghella, Tonello and Damjanić (1998)].

2.2 Strain measures

We can define the relative deformation gradient at φ_0 as a linear map $\mathbf{F} : T_{\varphi_0}\mathcal{C} \to T_{\varphi}\mathcal{C}$, which is mapping vector fields defined on the reference mid-surface onto the vector fields defined on the current mid-surface. $\mathbf{F}$ is given as

$$\mathbf{F} = \mathbf{t}_i \otimes \mathbf{g}^i = \mathbf{t}_{\,\alpha} \otimes \mathbf{g}^{\,\alpha} + \mathbf{t}_3 \otimes \mathbf{g}^3 \tag{7}$$

where $\mathbf{g}^{\,\alpha}$ are the dual base vectors defined trough the relationship $\mathbf{g}_{\,\alpha} \cdot \mathbf{g}^{\,\beta} = \delta^{\,\beta}_{\alpha}$, where $\delta^{\,\beta}_{\alpha}$ is the Kronecker symbol. We note that due to the choice of normal coordinates $\mathbf{g}^3 = \mathbf{g}_3$. By making use of the relative deformation gradient, the relative Lagrangian strain measures for the shell may be defined as

$$\mathbf{E}^{m,s} = \frac{1}{2}\left[\mathbf{F}^T\mathbf{F} - \mathbf{1}\right] \tag{8}$$

where $\mathbf{1}$ is a unit tensor relative to the reference configuration. It follows from (7) and (8) that the components of the strain tensor $\mathbf{E}^{m,s}$ may be written as

$$\varepsilon_{\alpha\beta} = \frac{1}{2}\left(\boldsymbol{\varphi}_{,\alpha} \cdot \boldsymbol{\varphi}_{,\beta} - \boldsymbol{\varphi}_{0,\alpha} \cdot \boldsymbol{\varphi}_{0,\beta}\right) \tag{9}$$

$$2\varepsilon_{\alpha 3} = \gamma_{\,\alpha} = \boldsymbol{\varphi}_{,\alpha} \cdot \mathbf{t} - \boldsymbol{\varphi}_{0,\alpha} \cdot \mathbf{t}_0 \tag{10}$$

where $\varepsilon_{\alpha\beta}$ and $\gamma_{\,\alpha}$ are the classical expressions for the membrane and the shear strains; e.g. see [Naghdi (1972)]. The Lagrangian strain measures for the bending strains can be developed by making use of the director gradient. By defining tensor $\mathbf{G} = \mathbf{t}_{,\alpha} \otimes \mathbf{g}^{\,\alpha}$ we may write

$$\mathbf{E}^b = \mathbf{F}^T\mathbf{G} - \mathbf{B}$$

where $\mathbf{B} = (\mathbf{g}_\alpha \cdot \mathbf{g}_{,\beta})\,\mathbf{g}^{\,\alpha} \otimes \mathbf{g}^{\,\beta}$ is the curvature tensor of the shell surface at the reference configuration. The components of the strain tensor $\mathbf{E}^b$ are then

$$\kappa_{\alpha\beta} = \boldsymbol{\varphi}_{,\alpha} \cdot \mathbf{t}_{,\beta} - \boldsymbol{\varphi}_{0,\alpha} \cdot \mathbf{t}_{0,\beta} \tag{11}$$

which are the classical expressions for the shell bending strains; e.g. see [Naghdi (1972)].

2.3 Constitutive relations

With the strain measures (9), (10) and (11) we can define the strain energy function by the following expression

$$\Phi\left(\varepsilon_{\alpha\beta}, \gamma_{\,\alpha}, \kappa_{\alpha\beta}, \cdot\right) \tag{12}$$

where an empty slot in (12) indicates that such a strain energy function should also depend upon the first and the second fundamental forms of the mid-surface. The effective stress resultants can be obtained as the corresponding partial derivatives of the strain energy, i.e.

$$n^{\alpha\beta} = \frac{\partial\Phi}{\partial\varepsilon_{\alpha\beta}}, \quad q^{\,\alpha} = \frac{\partial\Phi}{\partial\gamma_{\,\alpha}}, \quad m^{\alpha\beta} = \frac{\partial\Phi}{\partial\kappa_{\alpha\beta}} \tag{13}$$

The simplest properly invariant constitutive relations for shells are obtained by postulating small strains and isotropic shells, neglecting variation of metrics trough the shell thickness and assuming a quadratic form of the strain energy

$$n^{\alpha\beta} = \frac{Eh}{1-\nu^2} H^{\alpha\beta\gamma\delta}\varepsilon_{\gamma\delta}, \quad m^{\alpha\beta} = \frac{Eh^3}{12\,(1-\nu^2)} H^{\alpha\beta\gamma\delta}\kappa_{\gamma\delta}, \quad q^{\,\alpha} = \kappa G h g^{\alpha\beta}\gamma_{\,\beta} \tag{14}$$

where E is Young's modulus, ν is Poisson's ratio, κ is shear correction factor, $n^{\alpha\beta}$, $q^{\,\alpha}$ and $m^{\alpha\beta}$ are effective stress resultants and couples, $g^{\alpha\beta} = \mathbf{g}^{\,\alpha} \cdot \mathbf{g}^{\,\beta}$, and

$$H^{\alpha\beta\gamma\delta} = \nu g^{\alpha\beta} g^{\gamma\delta} + \frac{1}{2}\,(1-\nu)\left(g^{\alpha\gamma} g^{\beta\delta} + g^{\alpha\delta} g^{\beta\gamma}\right) \tag{15}$$

Remark 2. In order to simplify finite element implementation one usually introduces local Cartesian coordinates at the numerical integration points which simplify tensor (15), since for orthonormal frames $g^{\alpha\beta} = \delta^{\alpha\beta}$.

2.4 Kinetic energy

Kinetic energy for a shell is given by the expression

$$K = \frac{1}{2}\int_A \left[A_{\,\rho}\dot{\boldsymbol{\varphi}} \cdot \dot{\boldsymbol{\varphi}} + I_{\,\rho}\dot{\mathbf{t}} \cdot \dot{\mathbf{t}}\right] d\mathcal{A} \tag{16}$$

where $A_{\,\rho}$ and $I_{\,\rho}$ are the surface mass density and the rotation inertia of the shell-director, respectively, at the initial configuration. From the three-dimensional point of view $A_{\,\rho}$ and

I_ρ may be interpreted as the zeroth and the second moment of the mass density about the mid-surface (see e.g. [Brank, Briseghella, Tonello and Damjanić (1998)]) given by

$$A_\rho = \int_{h^-}^{h^+} \rho\mu d\zeta \approx \rho h \tag{17}$$

$$I_\rho = \int_{h^-}^{h^+} \rho\zeta^2\mu d\zeta \approx \rho\frac{h^3}{12} \tag{18}$$

Here, ρ is a three dimensional mass density. Geometric term $\mu = \sqrt{g^*}/\sqrt{g}$ is defined with g^* (3d Jacobian determinant of the map $\boldsymbol{\varphi}_0 + \zeta\mathbf{t}_0$) and $g = \det[\mathbf{g}_\alpha \cdot \mathbf{g}_\beta]$; $\sqrt{g} = \|\mathbf{g}_1 \times \mathbf{g}_2\|$, which is the measure of the mid-surface at the reference configuration. For thin shells it may be assumed that $\mu = 1$.

REMARK 3. We note in passing that the moment of inertia relative to the shell mid-surface is simply a scalar value, which is certainly easier to deal with than the inertia tensor which is found in 3d beam dynamics; e.g. see [Ibrahimbegović and Al Mikdad (1998), Al Mikdad and Ibrahimbegović (1997)].

2.5 Strong and weak form of balance equations

Two-dimensional momentum balance equations for geometrically exact shells take the following form (e.g. [Simo and Fox (1989)])

$$A_{\overline{\rho}}\ddot{\boldsymbol{\varphi}} = \frac{1}{\sqrt{a}}\left(\sqrt{a}\mathbf{n}^\alpha\right)_{,\alpha} + \overline{\mathbf{n}} \tag{19}$$

$$I_{\overline{\rho}}\left(\mathbf{t}\times\ddot{\mathbf{t}}\right) = \frac{1}{\sqrt{a}}\left(\sqrt{a}\mathbf{m}^\alpha\right)_{,\alpha} + \boldsymbol{\varphi}_{,\alpha}\times\mathbf{n}^\alpha + \overline{\mathbf{m}} \tag{20}$$

where $\mathbf{n}^\alpha$ are stress resultants (the components of $\mathbf{n}^\alpha$ are $n^{\alpha\beta}$ and $n^{\alpha 3} = q^\alpha$), $\mathbf{m}^\alpha$ are stress couples (the components of $\mathbf{m}^\alpha$ are $m^{\alpha\beta}$ and $m^{\alpha 3} = 0$), $\overline{\mathbf{n}}$ and $\overline{\mathbf{m}}$ are the applied forces and couples, respectively, $\sqrt{a} = \|\mathbf{t}_1 \times \mathbf{t}_2\|$ is the surface Jacobian at the deformed configuration, $a = \det[\mathbf{t}_\alpha \cdot \mathbf{t}_\beta]$. In (20) above $A_{\overline{\rho}}$ and $I_{\overline{\rho}}$ are the surface mass density and the rotation inertia of the shell-director, respectively, at the deformed configuration

In following D'Alambert principle, we can derive the corresponding weak form of the balance equations by introducing the 'inertia' forces, multiplying the equations by test functions $\delta\boldsymbol{\varphi}$ and $\delta\mathbf{t}$ and making use of the integration by parts; e.g. see [Hughes (1987)]. The weak form of the equations of motion may be then written with respect to the reference configuration as

$$\delta\Pi\left(\boldsymbol{\varphi},\mathbf{t},\delta\boldsymbol{\varphi},\delta\mathbf{t}\right) = \int_A \left(A_\rho\ddot{\boldsymbol{\varphi}}\cdot\delta\boldsymbol{\varphi} + I_\rho\ddot{\mathbf{t}}\cdot\delta\mathbf{t}\right)dA + \delta\Pi_{stat} = \delta\Pi_{dyn} + \delta\Pi_{stat} = 0 \tag{21}$$

$\delta\Pi_{stat}$ is the weak form of static equilibrium equations

$$\begin{array}{rcl}\delta\Pi_{stat} & = & \int_A \left[n^{\alpha\beta}\frac{1}{2}\left(\delta\boldsymbol{\varphi}_{,\alpha}\cdot\boldsymbol{\varphi}_{,\beta} + \boldsymbol{\varphi}_{,\alpha}\cdot\delta\boldsymbol{\varphi}_{,\beta}\right) + q^\alpha\left(\delta\boldsymbol{\varphi}_{,\alpha}\cdot\mathbf{t} + \boldsymbol{\varphi}_{,\alpha}\cdot\delta\mathbf{t}\right)\right. \\ & + & \left.\int_A m^{\alpha\beta}\left(\delta\boldsymbol{\varphi}_{,\alpha}\cdot\mathbf{t}_{,\beta} + \boldsymbol{\varphi}_{,\alpha}\cdot\delta\mathbf{t}_{,\beta}\right)\right]dA - \delta\Pi_{ext}\end{array} \tag{22}$$

where $\delta\Pi_{ext}$ is the virtual work of the applied forces, A is mid-surface area at the initial configuration, while $n^{\alpha\beta}$, q^α and $m^{\alpha\beta}$ are effective stress resultants and couples. $\delta\boldsymbol{\varphi}$ is an arbitrary test function which represents virtual displacements of the mid-surface, and $\delta\mathbf{t}$ is test function for shell-director vector, which must satisfy the orthogonality condition

$$\delta\mathbf{t}\cdot\mathbf{t} = 0 \tag{23}$$

emerging from the shell-director incompressibility assumption (2).

In solving the finite element approximation of equation (21) by the Newton incremental-iterative method, one makes use of the linearized form given as

$$\begin{aligned}
\mathrm{Lin}[\delta\Pi(\cdot)] &= [\delta\Pi(\cdot)] + \int_A \Big[\tfrac{1}{2} \left(\delta\boldsymbol{\varphi}_{,\alpha} \cdot \boldsymbol{\varphi}_{,\beta} + \boldsymbol{\varphi}_{,\alpha} \cdot \delta\boldsymbol{\varphi}_{,\beta} \right) \tfrac{\partial^2 \Phi}{\partial \varepsilon_{\alpha\beta} \partial \varepsilon_{\gamma\delta}} \tfrac{1}{2} \left(\Delta\boldsymbol{\varphi}_{,\gamma} \cdot \boldsymbol{\varphi}_{,\delta} + \boldsymbol{\varphi}_{,\gamma} \cdot \Delta\boldsymbol{\varphi}_{,\delta} \right) \\
&+ \left(\delta\boldsymbol{\varphi}_{,\alpha} \cdot \mathbf{t} + \boldsymbol{\varphi}_{,\alpha} \cdot \delta\mathbf{t} \right) \tfrac{\partial^2 \Phi}{\partial \gamma_\alpha \partial \gamma_\beta} \left(\Delta\boldsymbol{\varphi}_{,\beta} \cdot \mathbf{t} + \boldsymbol{\varphi}_{,\beta} \cdot \Delta\mathbf{t} \right) \\
&+ \left(\delta\boldsymbol{\varphi}_{,\alpha} \cdot \mathbf{t}_{,\beta} + \boldsymbol{\varphi}_{,\alpha} \cdot \delta\mathbf{t}_{,\beta} \right) \tfrac{\partial^2 \Phi}{\partial \kappa_{\alpha\beta} \partial \kappa_{\gamma\delta}} \left(\Delta\boldsymbol{\varphi}_{,\gamma} \cdot \mathbf{t}_{,\delta} + \boldsymbol{\varphi}_{,\gamma} \cdot \Delta\mathbf{t}_{,\delta} \right) \Big] \, dA \\
&+ \int_A \Big[n^{\alpha\beta} \tfrac{1}{2} \left(\delta\boldsymbol{\varphi}_{,\alpha} \cdot \Delta\boldsymbol{\varphi}_{,\beta} + \Delta\boldsymbol{\varphi}_{,\alpha} \cdot \delta\boldsymbol{\varphi}_{,\beta} \right) + q^\alpha \left(\delta\boldsymbol{\varphi}_{,\alpha} \cdot \Delta\mathbf{t} + \Delta\boldsymbol{\varphi}_{,\alpha} \cdot \delta\mathbf{t} \right) \\
&+ m^{\alpha\beta} \left(\delta\boldsymbol{\varphi}_{,\alpha} \cdot \Delta\mathbf{t}_{,\beta} + \Delta\boldsymbol{\varphi}_{,\alpha} \cdot \delta\mathbf{t}_{,\beta} \right) \\
&+ q^\alpha \left(\boldsymbol{\varphi}_{,\alpha} \cdot \Delta\delta\mathbf{t} \right) + m^{\alpha\beta} \left(\boldsymbol{\varphi}_{,\alpha} \cdot \Delta\delta\mathbf{t}_{,\beta} \right) \Big] \, dA \\
&+ \int_A \left(A_\rho \Delta\ddot{\boldsymbol{\varphi}} \cdot \delta\boldsymbol{\varphi} + I_\rho \Delta\ddot{\mathbf{t}} \cdot \delta\mathbf{t} + I_\rho \ddot{\mathbf{t}} \cdot \Delta\delta\mathbf{t} \right) dA = 0
\end{aligned} \tag{24}$$

where $\Delta\boldsymbol{\varphi}$ is incremental displacement vector and $\Delta\mathbf{t}$ is incremental director vector, constrained by $\Delta\mathbf{t} \cdot \mathbf{t} = 0$. Note, that $\Delta\delta\boldsymbol{\varphi}$ is zero, while $\Delta\delta\mathbf{t}$ is generally not. The integrals given in (24) provide basis for computing material, geometric and mass part of symmetric tangent operator. For discussion on symmetry of tangent operator for shells with finite rotations see e.g. [Suetake, Iura and Atluri (2001)].

2.6 Finite element interpolations

The spatial discretization of the problem is performed by an isoparametric finite element approximation. The following interpolations, referred to as the continuum-consistent, are used to approximate the shell geometry at any time $t \in [0, T]$

$$\boldsymbol{\varphi}\left(\xi^1, \xi^2, t\right) = \sum_{a=1}^{n_{en}} N_a\left(\xi^1, \xi^2\right) \boldsymbol{\varphi}_a(t), \quad \mathbf{t}\left(\xi^1, \xi^2, t\right) = \sum_{a=1}^{n_{en}} N_a\left(\xi^1, \xi^2\right) \mathbf{t}_a(t) \tag{25}$$

$N_a\left(\xi^1, \xi^2\right)$ are the corresponding shape functions for a shell element with n_{en} nodes, $\left(\xi^1, \xi^2\right) \in [-1, 1] \times [-1, 1]$, and $(\circ)_a$ are the corresponding nodal values. The virtual and incremental quantities at any time $t \in [0, T]$ are interpolated in the same manner

$$\delta\boldsymbol{\varphi}\left(\xi^1, \xi^2\right) = \sum_{a=1}^{n_{en}} N_a\left(\xi^1, \xi^2\right) \delta\boldsymbol{\varphi}_a, \quad \delta\mathbf{t}\left(\xi^1, \xi^2\right) = \sum_{a=1}^{n_{en}} N_a\left(\xi^1, \xi^2\right) \delta\mathbf{t}_a \tag{26}$$

$$\begin{aligned}
\Delta\boldsymbol{\varphi}\left(\xi^1, \xi^2\right) &= \sum_{a=1}^{n_{en}} N_a\left(\xi^1, \xi^2\right) \Delta\boldsymbol{\varphi}_a, \quad \Delta\mathbf{t}\left(\xi^1, \xi^2\right) = \sum_{a=1}^{n_{en}} N_a\left(\xi^1, \xi^2\right) \Delta\mathbf{t}_a \\
\Delta\delta\mathbf{t}\left(\xi^1, \xi^2\right) &= \sum_{a=1}^{n_{en}} N_a\left(\xi^1, \xi^2\right) \Delta\delta\mathbf{t}_a
\end{aligned} \tag{27}$$

The derivatives of the above interpolated functions with respect to time, t, or coordinates ξ^1 and ξ^2 may be easily obtained.

The interpolation of the transverse shear fields is based on the assumed strain method as suggested by [Dvorkin and Bathe (1984)]; the variational justification of that method may be found in [Simo and Hughes (1986)]. The assumed strain interpolations can be directly expressed by judiciously chosen displacement and rotation parameters, so that without lost of generality we can in the following present the problem as the displacement-based.

REMARK 4. In the present formulation we interpolate the components of the shell director vector. Discussion on more elaborate interpolation - where rotation parameters are directly interpolated - may be found in [Başar and Kintzel (2001)] for shells and [Zupan and Saje (2001)] for beams.

3 Shell director motion in terms of constrained finite rotation parameters and their time derivatives

3.1 Shell-director position

Let us consider a motion of the director vector attached to a particular point of the shell mid-surface. Since the director vector is of unit length, see (2), its position at any time $t \in [t_0, T]$ may be given by the finite rotation of the base vector $\mathbf{e} \equiv \mathbf{e}_3 = \{0, 0, 1\}^T$ (see Figure 1), thus having

$$\mathbf{t} = \mathbf{\Lambda}\mathbf{e}, \qquad \mathbf{t}_0 = \mathbf{\Lambda}_0\mathbf{e} \tag{28}$$

where $\mathbf{t}_0$ is the reference position of the director vector at the initial time $t = t_0$ and $\mathbf{\Lambda}_0 = \mathbf{\Lambda}_{|t=t_0}$.

In (28) the director vector position is described by an orthogonal tensor $\mathbf{\Lambda}$ which is an element of $SO(3)$ group

$$SO(3) = \{\mathbf{\Lambda} : \mathbb{R}^3 \to \mathbb{R}^3 \mid \mathbf{\Lambda}\mathbf{\Lambda}^T = \mathbf{I}, \det \mathbf{\Lambda} = 1\} \tag{29}$$

The principal difficulty introduced by describing the shell-director position by the rotation tensor $\mathbf{\Lambda}$ is due to the fact that $SO(3)$ is not a linear space. Therefore the issues of theoretical formulation, consistent linearization and update procedure become more complex. One can simplify the problem by exploiting the relations between the rotation tensor and its eigenvector. Namely, any rotation tensor $\mathbf{\Lambda}$ is associated with a skew-symmetric tensor $\mathbf{\Theta}$ trough an exponential mapping $\mathbf{\Lambda} = \exp[\mathbf{\Theta}]$, and any $\mathbf{\Theta}$ further possesses its axial vector $\boldsymbol{\vartheta}$, referred to as the rotation vector, such that $\mathbf{\Theta}\mathbf{b} = \boldsymbol{\vartheta} \times \mathbf{b}$, $\forall \mathbf{b} \in \mathbb{R}^3$. Given the rotation vector $\boldsymbol{\vartheta}$, one can reconstruct the corresponding orthogonal tensor $\mathbf{\Lambda}$ by using either the exponential mapping or the Rodrigues formula; see e.g. [Simo and Fox (1989)] and references therein

$$\mathbf{\Lambda} = \tilde{\mathbf{\Lambda}}(\boldsymbol{\vartheta}) = \exp[\mathbf{\Theta}] \tag{30}$$

$$\mathbf{\Lambda} = \tilde{\mathbf{\Lambda}}(\boldsymbol{\vartheta}) = \cos\vartheta\mathbf{I} + \frac{\sin\vartheta}{\vartheta}\mathbf{\Theta} + \frac{1-\cos\vartheta}{\vartheta^2}\boldsymbol{\vartheta}\otimes\boldsymbol{\vartheta} \tag{31}$$

Here $\tilde{\mathbf{\Lambda}}(\boldsymbol{\alpha})$ denotes rotation defined by rotation vector $\boldsymbol{\alpha}$ and expressed either in form (30) or (31). It will be clear from the context which form is used.

$\mathbf{\Lambda}$ may be viewed as a composition of two orthogonal tensors, one taking us from the fixed global basis to the local basis in the reference configuration and another taking us further to the current configuration. One may rewrite the equation of shell-director motion, (28), as

$$\mathbf{t} = \mathbf{\Lambda}\mathbf{e} = \mathbf{\Lambda}_0\tilde{\mathbf{\Lambda}}(\boldsymbol{\vartheta})\,\mathbf{e} \tag{32}$$

$$\mathbf{t} = \mathbf{\Lambda}\mathbf{e} = \tilde{\mathbf{\Lambda}}(\boldsymbol{\theta})\,\mathbf{\Lambda}_0\mathbf{e} = \tilde{\mathbf{\Lambda}}(\boldsymbol{\theta})\,\mathbf{t}_0 \tag{33}$$

We refer to $\boldsymbol{\vartheta}$ as the material rotation vector, while $\boldsymbol{\theta}$ represents its spatial counterpart[1]; motivation for this notation is explained in [Ibrahimbegović, Frey and Kožar (1995)]. Their mutual

[1] In this section $\boldsymbol{\vartheta}$ and $\boldsymbol{\theta}$ represent the total material and the total spatial rotation vector, respectively, which are measured from the reference configuration, while in Section 4 the corresponding incremental rotation vectors, which are reset at the begining of each solution increment, will be introduced.

relationship follows from (32) and (33) as

$$\tilde{\mathbf{\Lambda}}\left(\boldsymbol{\vartheta}\right)=\mathbf{\Lambda}_0^T\tilde{\mathbf{\Lambda}}\left(\boldsymbol{\theta}\right)\mathbf{\Lambda}_0\Rightarrow\boldsymbol{\theta}=\mathbf{\Lambda}_0\boldsymbol{\vartheta} \tag{34}$$

$$\tilde{\mathbf{\Lambda}}\left(\boldsymbol{\theta}\right)=\mathbf{\Lambda}_0\tilde{\mathbf{\Lambda}}\left(\boldsymbol{\vartheta}\right)\mathbf{\Lambda}_0^T\Rightarrow\boldsymbol{\vartheta}=\mathbf{\Lambda}_0^T\boldsymbol{\theta} \tag{35}$$

Let us assume that $\tilde{\mathbf{\Lambda}}\left(\boldsymbol{\vartheta}\right)$ and $\tilde{\mathbf{\Lambda}}\left(\boldsymbol{\theta}\right)$ rotate $\mathbf{e}$ and $\mathbf{t}_0$, respectively, without drilling rotation. In other words, rotations $\tilde{\mathbf{\Lambda}}\left(\boldsymbol{\vartheta}\right)$ and $\tilde{\mathbf{\Lambda}}\left(\boldsymbol{\theta}\right)$ are constrained by requiring that the rotation vector component along the rotated vector plays no role in the theory. Rotation vector is therefore perpendicular to both initial and rotated vector

$$\text{Eq. (32)}\Rightarrow\boldsymbol{\vartheta}\cdot\mathbf{e}=0,\quad\boldsymbol{\vartheta}\cdot\mathbf{\Lambda}_0^T\mathbf{t}=0 \tag{36}$$

$$\text{Eq. (33)}\Rightarrow\boldsymbol{\theta}\cdot\mathbf{t}_0=0,\quad\boldsymbol{\theta}\cdot\mathbf{t}=0 \tag{37}$$

From (28) and (34) it follows immediately that the constraints $(36)_1$ and $(37)_1$ are equivalent, as well as $(36)_2$ and $(37)_2$. It also follows from (36), that the material rotational vector always lies in the plane defined by fixed vectors $\mathbf{e}_1$ and $\mathbf{e}_2$, or, in interpretation of $(37)_1$, in the plane tangential to the mid-surface at the reference configuration.

3.2 Shell-director velocity

Velocity of the shell-director vector $\mathbf{t}$ at any time $t\in[t_0,T]$ may be formally obtained as

$$\dot{\mathbf{t}}=\frac{d}{dt}\,|_{t=0}\,\mathbf{t}_t=\frac{d}{dt}\,|_{t=0}\,\left[\mathbf{\Lambda}_t\right]\mathbf{e} \tag{38}$$

We will derive explicit expressions of the shell-director velocity by defining a one parameter family of shell-director vectors $t\rightarrow\mathbf{t}_t$ in four different ways, depending on the definition of a one parameter family of constrained rotations $t\rightarrow\mathbf{\Lambda}_t$.

3.2.1 Multiplicative update of constrained rotations

Let us multiply $\mathbf{\Lambda}$ from the right hand side with an orthogonal tensor $\exp\left[t\dot{\mathbf{\Psi}}\right]$ to get

$$\mathbf{t}_t=\mathbf{\Lambda}_t\mathbf{e}=\mathbf{\Lambda}\exp\left[t\dot{\mathbf{\Psi}}\right]\mathbf{e} \tag{39}$$

By analogy, multiplication of $\mathbf{\Lambda}$ from the left hand side with an orthogonal tensor $\exp\left[t\dot{\mathbf{W}}\right]$ gives

$$\mathbf{t}_t=\mathbf{\Lambda}_t\mathbf{e}=\exp\left[t\dot{\mathbf{W}}\right]\mathbf{\Lambda}\mathbf{e}=\exp\left[t\dot{\mathbf{W}}\right]\mathbf{t} \tag{40}$$

$\dot{\mathbf{\Psi}}$ and $\dot{\mathbf{W}}$ are skew-symmetric tensors defining material and spatial angular velocities of the shell-director motion, respectively.

From (39) and (40) we can express time derivative of $\mathbf{\Lambda}$ as

$$\dot{\mathbf{\Lambda}}=\frac{d}{dt}\,|_{t=0}\,\mathbf{\Lambda}_t=\mathbf{\Lambda}\dot{\mathbf{\Psi}}=\dot{\mathbf{W}}\mathbf{\Lambda} \tag{41}$$

Mutual relationship between $\dot{\mathbf{\Psi}}$ and $\dot{\mathbf{W}}$

$$\dot{\mathbf{\Psi}}=\mathbf{\Lambda}^T\dot{\mathbf{W}}\mathbf{\Lambda},\quad\dot{\mathbf{W}}=\mathbf{\Lambda}\dot{\mathbf{\Psi}}\mathbf{\Lambda}^T \tag{42}$$

further leads to the corresponding relationship between their axial vectors [Ibrahimbegović, Frey and Kožar (1995)]

$$\dot{\boldsymbol{\psi}} = \boldsymbol{\Lambda}^T \dot{\mathbf{w}}, \quad \dot{\mathbf{w}} = \boldsymbol{\Lambda} \dot{\boldsymbol{\psi}} \tag{43}$$

By using (38) we get from (39) and (40) the following expressions for the shell-director velocity in terms of $\dot{\boldsymbol{\psi}}$ and $\dot{\mathbf{w}}$

$$\dot{\mathbf{t}} = \boldsymbol{\Lambda} \left(\dot{\boldsymbol{\psi}} \times \mathbf{e} \right) \tag{44}$$

$$\dot{\mathbf{t}} = \dot{\mathbf{w}} \times \boldsymbol{\Lambda} \mathbf{e} = \dot{\mathbf{w}} \times \mathbf{t} \tag{45}$$

Exploiting the analogy between (32) and (39), we may conclude (see (36)) that the axial vector $\dot{\boldsymbol{\psi}}$ is constrained as

$$\dot{\boldsymbol{\psi}} \cdot \mathbf{e} = 0 \tag{46}$$

while, in the same manner, we may observe from (33) and (40) that the axial vector $\dot{\mathbf{w}}$ is constrained as

$$\dot{\mathbf{w}} \cdot \mathbf{t} = 0 \tag{47}$$

3.2.2 Additive update of constrained rotations

The third and the fourth possibility for the construction of $\mathbf{t}_t$ in (38) exploit the additive update of rotational parameters. By using the material rotation vector $\boldsymbol{\vartheta}$ we have

$$\mathbf{t}_t = \boldsymbol{\Lambda}_t \mathbf{e} = \boldsymbol{\Lambda}_0 \tilde{\boldsymbol{\Lambda}} \left(\boldsymbol{\vartheta} + t \dot{\boldsymbol{\vartheta}} \right) \mathbf{e} \tag{48}$$

while with its spatial counterpart $\boldsymbol{\theta}$ we obtain

$$\mathbf{t}_t = \tilde{\boldsymbol{\Lambda}} \left(\boldsymbol{\theta} + t \dot{\boldsymbol{\theta}} \right) \boldsymbol{\Lambda}_0 \mathbf{e} = \tilde{\boldsymbol{\Lambda}} \left(\boldsymbol{\theta} + t \dot{\boldsymbol{\theta}} \right) \mathbf{t}_0 \tag{49}$$

Time derivative of (48) and (49) leads to the expressions of the shell-director velocity in terms of the rotational vectors $\boldsymbol{\vartheta}$ and $\boldsymbol{\theta}$ and their velocities:

$$\dot{\mathbf{t}} = \boldsymbol{\Lambda}_0 \mathbf{A}^{\vartheta} \, \dot{\boldsymbol{\vartheta}} \tag{50}$$

$$\dot{\mathbf{t}} = \mathbf{A}^{\theta} \, \dot{\boldsymbol{\theta}} \tag{51}$$

with

$$\mathbf{A}^{\vartheta} = \left[-\frac{\sin \vartheta}{\vartheta} \left(\mathbf{e} \otimes \boldsymbol{\vartheta} + \mathbf{E} \right) + \frac{\vartheta \cos \vartheta - \sin \vartheta}{\vartheta^3} \left(\boldsymbol{\vartheta} \times \mathbf{e} \right) \otimes \boldsymbol{\vartheta} \right] \tag{52}$$

where $\vartheta = \|\boldsymbol{\vartheta}\|$ and $\mathbf{E}\mathbf{b} = \mathbf{e} \times \mathbf{b}, \forall \, \mathbf{b} \in \mathbb{R}^3$, and

$$\mathbf{A}^{\theta} = \left[-\frac{\sin \theta}{\theta} \left(\mathbf{t}_0 \otimes \boldsymbol{\theta} + \mathbf{T}_0 \right) + \frac{\theta \cos \theta - \sin \theta}{\theta^3} \left(\boldsymbol{\theta} \times \mathbf{t}_0 \right) \otimes \boldsymbol{\theta} \right] \tag{53}$$

where $\theta = \|\boldsymbol{\theta}\|$ and $\mathbf{T}_0 \mathbf{b} = \mathbf{t}_0 \times \mathbf{b}, \forall \mathbf{b} \in \mathbb{R}^3$. $\mathbf{A}^{\vartheta}$ and $\mathbf{A}^{\theta}$ are obtained by using (31) in (48) and (49), and by observing that $(\boldsymbol{\vartheta} \otimes \boldsymbol{\vartheta}) \, \mathbf{e} = \mathbf{0}$ and $(\boldsymbol{\theta} \otimes \boldsymbol{\theta}) \, \mathbf{t}_0 = \mathbf{0}$ which follows from (36) and (37). Some further details of the derivation of the above tensors may be found in [Brank, Perić and Damjanić (1997) and Ibrahimbegović, Brank and Courtois (2001)].

The relation between $\dot{\boldsymbol{\vartheta}}$ and $\dot{\boldsymbol{\theta}}$ comes from the time derivative of (34) and (35)

$$\dot{\boldsymbol{\theta}} = \boldsymbol{\Lambda}_0 \dot{\boldsymbol{\vartheta}}, \quad \dot{\boldsymbol{\vartheta}} = \boldsymbol{\Lambda}_0^T \dot{\boldsymbol{\theta}} \tag{54}$$

while by using (50), (51) and (54) we may obtain

$$\mathbf{A}^{\theta} = \mathbf{\Lambda}_0 \mathbf{A}^{\vartheta} \mathbf{\Lambda}_0^T \tag{55}$$

It also follows trivially from (36) and (37) that

$$\dot{\boldsymbol{\vartheta}} \cdot \mathbf{e} = 0 \Longleftrightarrow \dot{\boldsymbol{\theta}} \cdot \mathbf{t}_0 = 0 \tag{56}$$

$$\dot{\boldsymbol{\theta}} \cdot \mathbf{t} = 0, \quad \boldsymbol{\theta} \cdot \dot{\mathbf{t}} = 0 \tag{57}$$

Further developments and commutative diagrams providing relations between the parameters introduced above ($\dot{\boldsymbol{\psi}}$, $\dot{\mathbf{w}}$, $\dot{\boldsymbol{\vartheta}}$ and $\dot{\boldsymbol{\theta}}$) are presented in [Brank and Ibrahimbegović (2001)].

REMARK 5. By multiplying $\dot{\mathbf{t}}$ with $\mathbf{t}$, we have $\dot{\mathbf{t}} \cdot \mathbf{t} = 0$, the condition which follows from the incompressibility assumption (2) of the shell-director vector. It can be shown that the right had sides of (44), (45), (50) and (51) satisfy this condition.

3.3 Shell-director acceleration

Having concluded that we have four different possibilities to express velocity of the shell-director by using either exponential mapping formula or Rodrigues formula, we proceed by deriving expressions for the shell-director acceleration. By taking time derivative of (44), (45), (50) and (51) we have

$$\ddot{\mathbf{t}} = \dot{\mathbf{\Lambda}} \left(\dot{\boldsymbol{\psi}} \times \mathbf{e} \right) + \mathbf{\Lambda} \left(\ddot{\boldsymbol{\psi}} \times \mathbf{e} \right) \tag{58}$$

$$\ddot{\mathbf{t}} = \dot{\mathbf{w}} \times \dot{\mathbf{t}} + \ddot{\mathbf{w}} \times \mathbf{t} \tag{59}$$

$$\ddot{\mathbf{t}} = \mathbf{\Lambda}_0 \left[\mathbf{Y}^{\vartheta} \dot{\boldsymbol{\vartheta}} + \mathbf{A}^{\vartheta} \ddot{\boldsymbol{\vartheta}} \right] \tag{60}$$

$$\ddot{\mathbf{t}} = \mathbf{Y}^{\theta} \dot{\boldsymbol{\theta}} + \mathbf{A}^{\theta} \ddot{\boldsymbol{\theta}} \tag{61}$$

where $\mathbf{Y}^{\vartheta}$ is a tensor function of $\boldsymbol{\vartheta}$ and $\dot{\boldsymbol{\vartheta}}$ obtained by time derivative of (52)

$$\begin{aligned} \mathbf{Y}^{\vartheta} &= -\tfrac{\vartheta \cos\vartheta - \sin\vartheta}{\vartheta^3} \left(\boldsymbol{\vartheta} \cdot \dot{\boldsymbol{\vartheta}} \right) (\mathbf{e} \otimes \boldsymbol{\vartheta} + \mathbf{E}) - \tfrac{\sin\vartheta}{\vartheta} \mathbf{e} \otimes \dot{\boldsymbol{\vartheta}} \\ &+ \tfrac{\sin\vartheta \left(3 - \vartheta^2\right) - 3\vartheta\cos\vartheta}{\vartheta^5} \left(\boldsymbol{\vartheta} \cdot \dot{\boldsymbol{\vartheta}} \right) (\boldsymbol{\vartheta} \times \mathbf{e}) \otimes \boldsymbol{\vartheta} \\ &+ \tfrac{\vartheta \cos\vartheta - \sin\vartheta}{\vartheta^3} \left[\left(\dot{\boldsymbol{\vartheta}} \times \mathbf{e} \right) \otimes \boldsymbol{\vartheta} + (\boldsymbol{\vartheta} \times \mathbf{e}) \otimes \dot{\boldsymbol{\vartheta}} \right] \end{aligned} \tag{62}$$

and $\mathbf{Y}^{\theta}$ is a tensor function of $\boldsymbol{\theta}$ and $\dot{\boldsymbol{\theta}}$ obtained by time derivative of (53)

$$\begin{aligned} \mathbf{Y}^{\theta} &= -\tfrac{\theta \cos\theta - \sin\theta}{\theta^3} \left(\boldsymbol{\theta} \cdot \dot{\boldsymbol{\theta}} \right) (\mathbf{t}_0 \otimes \boldsymbol{\theta} + \mathbf{T}_0) - \tfrac{\sin\theta}{\theta} \mathbf{t}_0 \otimes \dot{\boldsymbol{\theta}} \\ &+ \tfrac{\sin\theta \left(3 - \theta^2\right) - 3\theta\cos\theta}{\theta^5} \left(\boldsymbol{\theta} \cdot \dot{\boldsymbol{\theta}} \right) (\boldsymbol{\theta} \times \mathbf{t}_0) \otimes \boldsymbol{\theta} \\ &+ \tfrac{\theta \cos\theta - \sin\theta}{\theta^3} \left[\left(\dot{\boldsymbol{\theta}} \times \mathbf{t}_0 \right) \otimes \boldsymbol{\theta} + (\boldsymbol{\theta} \times \mathbf{t}_0) \otimes \dot{\boldsymbol{\theta}} \right] \end{aligned} \tag{63}$$

Some details on the derivation of tensors $\mathbf{Y}^{\vartheta}$ and $\mathbf{Y}^{\theta}$ may be found in [Brank, Perić and Damjanić (1997)]. Expressions (58) and (59) can be further elaborated. By noting that $\dot{\mathbf{\Lambda}} = \mathbf{\Lambda} \dot{\mathbf{\Psi}}$ (see (41)) we get from (58)

$$\begin{aligned} \ddot{\mathbf{t}} &= \mathbf{\Lambda} \left[\dot{\boldsymbol{\psi}} \times \left(\dot{\boldsymbol{\psi}} \times \mathbf{e} \right) + \ddot{\boldsymbol{\psi}} \times \mathbf{e} \right] \\ &= \mathbf{\Lambda} \left[\dot{\boldsymbol{\psi}} \left(\dot{\boldsymbol{\psi}} \cdot \mathbf{e} \right) - \mathbf{e} \left(\dot{\boldsymbol{\psi}} \cdot \dot{\boldsymbol{\psi}} \right) + \ddot{\boldsymbol{\psi}} \times \mathbf{e} \right] = \mathbf{\Lambda} \left(-\mathbf{e} \dot{\psi}^2 + \ddot{\boldsymbol{\psi}} \times \mathbf{e} \right) \end{aligned} \tag{64}$$

where $\dot{\psi} = \left\| \dot{\boldsymbol{\psi}} \right\|$. By using $\dot{\mathbf{t}} = \dot{\mathbf{w}} \times \mathbf{t}$ in (59) and applying similar procedure as in (64) above, we have

$$\ddot{\mathbf{t}} = \dot{\mathbf{w}} \times (\dot{\mathbf{w}} \times \mathbf{t}) + \ddot{\mathbf{w}} \times \mathbf{t} = -\mathbf{t}\dot{w}^2 + \ddot{\mathbf{w}} \times \mathbf{t} \tag{65}$$

where $\dot{w} = \|\dot{\mathbf{w}}\|$. Note, that the absolute values of material and spatial angular velocities are equal, i.e. $\dot{\psi} = \dot{w}$.

Let us now check which constraints are acting on the acceleration of rotational parameters. Taking the time derivatives of (42) we get

$$\ddot{\mathbf{W}} = \ddot{\mathbf{\Lambda}}\mathbf{\Lambda}^T + \dot{\mathbf{\Lambda}}\dot{\mathbf{\Lambda}}^T, \quad \ddot{\mathbf{\Psi}} = \mathbf{\Lambda}^T\ddot{\mathbf{\Lambda}} + \dot{\mathbf{\Lambda}}^T\dot{\mathbf{\Lambda}} \tag{66}$$

It can be verified that angular acceleration tensors $\ddot{\mathbf{W}}$ and $\ddot{\mathbf{\Psi}}$ are both skew-symmetric, and that their mutual relationship can be written as

$$\ddot{\mathbf{W}} = \mathbf{\Lambda}\ddot{\mathbf{\Psi}}\mathbf{\Lambda}^T, \quad \ddot{\mathbf{\Psi}} = \mathbf{\Lambda}^T\ddot{\mathbf{W}}\mathbf{\Lambda} \tag{67}$$

We can also establish the mutual relationship of their axial vectors as

$$\ddot{\mathbf{w}} = \mathbf{\Lambda}\ddot{\boldsymbol{\psi}}, \quad \ddot{\boldsymbol{\psi}} = \mathbf{\Lambda}^T\ddot{\mathbf{w}} \tag{68}$$

It follows trivially from (46) that

$$\ddot{\boldsymbol{\psi}} \cdot \mathbf{e} = 0 \tag{69}$$

With the time differentiation of (47) we have $\ddot{\mathbf{w}} \cdot \mathbf{t} + \dot{\mathbf{w}} \cdot \dot{\mathbf{t}} = 0$, from which it further follows by using $\dot{\mathbf{w}} \cdot \dot{\mathbf{t}} = \dot{\mathbf{w}} \cdot (\dot{\mathbf{w}} \times \mathbf{t}) = 0$ that

$$\ddot{\mathbf{w}} \cdot \mathbf{t} = 0 \tag{70}$$

It also follows from (56) and (57) that

$$\ddot{\boldsymbol{\vartheta}} \cdot \mathbf{e} = 0 \Longleftrightarrow \ddot{\boldsymbol{\theta}} \cdot \mathbf{t}_0 = 0 \tag{71}$$

$$\ddot{\boldsymbol{\theta}} \cdot \mathbf{t} = 0, \quad \dot{\boldsymbol{\theta}} \cdot \dot{\mathbf{t}} = 0, \quad \boldsymbol{\theta} \cdot \ddot{\mathbf{t}} = 0 \tag{72}$$

3.4 Two versus three rotational parameters

In the coordinate representation of the rotation vector (which can be either material or spatial object), angular velocity of the shell-director motion $(\dot{\boldsymbol{\psi}}, \dot{\mathbf{w}})$, angular acceleration of the shell-director motion $(\ddot{\boldsymbol{\psi}}, \ddot{\mathbf{w}})$, velocity of the rotation vector $(\dot{\boldsymbol{\vartheta}}, \dot{\boldsymbol{\theta}})$ and acceleration of the rotation vector $(\ddot{\boldsymbol{\vartheta}}, \ddot{\boldsymbol{\theta}})$, one can exploit the constraints presented in the above sections.

However, we can only exploit constraints if known vectors (i.e. fixed base vectors or vectors associated with the reference configuration) appear in relations with the rotational parameters and their time derivatives. In other words, the constraints can be exploited to reduce the coordinate representation only with the material objects. The material rotational objects can be presented by two components, while on the other hand, their spatial counterparts have to be expressed by all three components which are not mutually independent.

The coordinate representation of the tensors defined above in section 3 are therefore either (3×3) matrices for tensors with spatial objects or (2×3), (3×2) and (2×2) matrices for tensors with material objects. Similarly, the coordinate representation of spatial vectors is of (3×1) form, while of material vectors is of (2×1) form.

Material and spatial objects associated with the rotation, velocity and acceleration of the shell-director vector are summarized in Table 1.

Table 1. Parameters of the shell-director motion, their time derivatives and related constraints.

	Material (2 comp.)	Constraint	Spatial (3 comp.)	Constraint
Total rotation vector	$\boldsymbol{\vartheta}$	(36)	$\boldsymbol{\theta}$	(37)
Angular velocity	$\dot{\boldsymbol{\psi}}$	(46)	$\dot{\mathbf{w}}$	(47)
Angular acceleration	$\ddot{\boldsymbol{\psi}}$	(69)	$\ddot{\mathbf{w}}$	(70)
Vel. of the total rotation vector	$\dot{\boldsymbol{\vartheta}}$	(56)	$\dot{\boldsymbol{\theta}}$	(57)
Acc. of the total rotation vector	$\ddot{\boldsymbol{\vartheta}}$	(71)	$\ddot{\boldsymbol{\theta}}$	(72)

4 Constrained incremental rotation vector

It has been noted [Betsch, Menzel and Stein (1998) and Ibrahimbegović, Brank and Courtois (2001)] that an attractive parametrization of constrained finite rotation with the total rotation vector ($\boldsymbol{\vartheta}$ or $\boldsymbol{\theta}$) will exhibit the singularity problem whenever its norm reaches a multiple of π. For overcoming this deficiency we introduce in this section an incremental rotation vector which, moreover, is fully consistent with the standard incremental solution scheme for nonlinear problems. Since it maintains additive iterative rotational updates it is also very suitable for optimization problems; see e.g. [Kegl (2000)], [Ibrahimbegović and Knopf-Lenoir (2001)].

4.1 Incremental rotation updates

The evolution of configuration space variables is obtained by a step-by-step integration scheme. The time interval of interest is partitioned into the number of time steps: $0 < t_1 < \ldots < t_n < t_{n+1} < \ldots < T$. At the typical time, t_n, the values of translational and rotational motion components are denoted as

$$\boldsymbol{\varphi}_n = \boldsymbol{\varphi}\left(t_n\right), \quad \mathbf{t}_n = \mathbf{t}\left(t_n\right) \tag{73}$$

where $\mathbf{t}_n$ is defined via orthogonal tensor $\boldsymbol{\Lambda}_n = \boldsymbol{\Lambda}\left(t_n\right)$ trough relation $\mathbf{t}_n = \boldsymbol{\Lambda}_n \mathbf{e}$.

Let us now substitute total rotation vectors $\boldsymbol{\vartheta}$ (material version) and $\boldsymbol{\theta}$ (spatial version) by the corresponding incremental rotation vectors $\boldsymbol{\vartheta}_{n+1}$ and $\boldsymbol{\theta}_{n+1}$, which are reset to zero at the beginning of each solution increment. Without going trough a detailed proof we can show that the relations for the position, velocity and acceleration of the shell-director vector given in section 3 also hold for the corresponding incremental rotation vector, simply by making the following substitutions

$$\begin{array}{rcl}
\boldsymbol{\vartheta}, \dot{\boldsymbol{\vartheta}}, \ddot{\boldsymbol{\vartheta}} & \rightarrow & \boldsymbol{\vartheta}_{n+1}, \dot{\boldsymbol{\vartheta}}_{n+1}, \ddot{\boldsymbol{\vartheta}}_{n+1} \\
\boldsymbol{\theta}, \dot{\boldsymbol{\theta}}, \ddot{\boldsymbol{\theta}} & \rightarrow & \boldsymbol{\theta}_{n+1}, \dot{\boldsymbol{\theta}}_{n+1}, \ddot{\boldsymbol{\theta}}_{n+1} \\
\boldsymbol{\Lambda}_0, \boldsymbol{\Lambda}, \mathbf{t}_0, \mathbf{t} & \rightarrow & \boldsymbol{\Lambda}_n, \boldsymbol{\Lambda}_{n+1}, \mathbf{t}_n, \mathbf{t}_{n+1} \\
\mathbf{A}^{\vartheta}, \mathbf{Y}^{\vartheta} & \rightarrow & \mathbf{A}^{\vartheta}_{n+1}, \mathbf{Y}^{\vartheta}_{n+1} \\
\mathbf{A}^{\theta}, \mathbf{Y}^{\theta} & \rightarrow & \mathbf{A}^{\theta}_{n+1}, \mathbf{Y}^{\theta}_{n+1}
\end{array} \tag{74}$$

In the context of step by step integration scheme, the new value of displacement vector at time t_{n+1} is obtained trivially as

$$\boldsymbol{\varphi}_{n+1} = \boldsymbol{\varphi}_n + \mathbf{u}_{n+1} \tag{75}$$

where $\mathbf{u}_{n+1} \equiv \Delta\boldsymbol{\varphi}_{n+1}$ are incremental displacements of the mid-surface point.

Obtaining $\mathbf{t}_{n+1}$ can be more complicated. Namely, to update the shell-director vector, one first needs to update the orthogonal matrix $\boldsymbol{\Lambda}_n$. Its incremental update can be carried out in terms of the incremental rotation vector as

$$\boldsymbol{\Lambda}_{n+1} = \tilde{\boldsymbol{\Lambda}}\left(\boldsymbol{\theta}_{n+1}\right)\boldsymbol{\Lambda}_n = \boldsymbol{\Lambda}_n \tilde{\boldsymbol{\Lambda}}\left(\boldsymbol{\vartheta}_{n+1}\right) \tag{76}$$

Considering that $\mathbf{\Lambda}_n$ is an orthogonal tensor, one may obtain the following relations from (76)

$$\tilde{\mathbf{\Lambda}}\left(\boldsymbol{\theta}_{n+1}\right) = \mathbf{\Lambda}_n \tilde{\mathbf{\Lambda}}\left(\boldsymbol{\vartheta}_{n+1}\right) \mathbf{\Lambda}_n^T, \qquad \tilde{\mathbf{\Lambda}}\left(\boldsymbol{\vartheta}_{n+1}\right) = \mathbf{\Lambda}_n^T \tilde{\mathbf{\Lambda}}\left(\boldsymbol{\theta}_{n+1}\right) \mathbf{\Lambda}_n \tag{77}$$

Furthermore, taking into account that a skew-symmetric tensor and the corresponding orthogonal tensor obtained by its exponentiation share the same eigenvectors [Ibrahimbegović, Frey and Kožar (1995)] it follows that

$$\boldsymbol{\theta}_{n+1} = \mathbf{\Lambda}_n \boldsymbol{\vartheta}_{n+1}, \qquad \boldsymbol{\vartheta}_{n+1} = \mathbf{\Lambda}_n^T \boldsymbol{\theta}_{n+1} \tag{78}$$

Having updated the orthogonal matrix $\mathbf{\Lambda}_n$ by using (76), we may proceed with the evaluation of the shell-director at time t_{n+1}. According to (76) we have two possibilities in terms of the incremental rotation vector

$$\mathbf{t}_{n+1} = \mathbf{\Lambda}_n \tilde{\mathbf{\Lambda}}\left(\boldsymbol{\vartheta}_{n+1}\right) \mathbf{e} \tag{79}$$

$$\mathbf{t}_{n+1} = \tilde{\mathbf{\Lambda}}\left(\boldsymbol{\theta}_{n+1}\right) \mathbf{\Lambda}_n \mathbf{e} = \tilde{\mathbf{\Lambda}}\left(\boldsymbol{\theta}_{n+1}\right) \mathbf{t}_n \tag{80}$$

By exploiting similarities of (32) and (33) with (79) and (80), respectively, we can conclude that $\boldsymbol{\vartheta}_{n+1}$ and $\boldsymbol{\theta}_{n+1}$ are subjected to the following constraints (see (36) and (37))

$$\boldsymbol{\vartheta}_{n+1} \cdot \mathbf{e} = 0, \qquad \boldsymbol{\vartheta}_{n+1} \cdot \mathbf{\Lambda}_n^T \mathbf{t}_{n+1} = 0 \tag{81}$$

$$\boldsymbol{\theta}_{n+1} \cdot \mathbf{t}_n = 0, \qquad \boldsymbol{\theta}_{n+1} \cdot \mathbf{t}_{n+1} = 0 \tag{82}$$

where, again, constraints $(81)_1$ and $(82)_1$ are equivalent. By using (74), the constraints (56) and (71) now turn to be

$$\dot{\boldsymbol{\vartheta}}_{n+1} \cdot \mathbf{e} = 0, \qquad \ddot{\boldsymbol{\vartheta}}_{n+1} \cdot \mathbf{e} = 0 \tag{83}$$

while the constraints associated with the time derivatives of $\boldsymbol{\theta}_{n+1}$ follow from (82).

4.2 Iterative rotation updates

When an implicit time-stepping scheme is used, the final values of the state variables at time increment $[t_n, t_{n+1}]$ are established by an iterative procedure carried over the increment. To that end, let superscript (i) denote the iteration counter.

At each iteration the incremental displacement update is performed in a standard additive fashion as

$$\mathbf{u}_{n+1}^{(i+1)} = \mathbf{u}_{n+1}^{(i)} + \Delta \mathbf{u}_{n+1}^{(i)} \tag{84}$$

where $\Delta \mathbf{u}_{n+1}^{(i)}$ is the (i)th contribution to the incremental displacement field.

The iterative values of the shell-director vector are obtained trough the corresponding iterative updates of the orthogonal tensor, $\mathbf{\Lambda}_{n+1}$, since

$$\mathbf{t}_{n+1}^{(i+1)} = \mathbf{\Lambda}_{n+1}^{(i+1)} \mathbf{e} \tag{85}$$

In the iterative update of finite rotations we can choose between spatial and material representations. By making use of the material form of the incremental rotation vector $\boldsymbol{\vartheta}_{n+1}^{(i)}$ and its iterative increment $\Delta \boldsymbol{\vartheta}_{n+1}^{(i)} = \Delta t^{(i)}\, \dot{\boldsymbol{\vartheta}}_{n+1}^{(i)}$ we have

$$\mathbf{\Lambda}_{n+1}^{(i+1)} = \mathbf{\Lambda}_n \tilde{\mathbf{\Lambda}} \left(\boldsymbol{\vartheta}_{n+1}^{(i)} + \Delta \boldsymbol{\vartheta}_{n+1}^{(i)} \right) \tag{86}$$

The rotation update can also be performed with the spatial rotation parameters as

$$\mathbf{\Lambda}_{n+1}^{(i+1)} = \tilde{\mathbf{\Lambda}} \left(\boldsymbol{\theta}_{n+1}^{(i)} + \Delta \boldsymbol{\theta}_{n+1}^{(i)} \right) \mathbf{\Lambda}_n \tag{87}$$

Comparing (86) and (87) the following relations may be obtained

$$\Delta\boldsymbol{\theta}_{n+1}^{(i)} = \boldsymbol{\Lambda}_n \Delta\boldsymbol{\vartheta}_{n+1}^{(i)} \tag{88}$$

Noting that the material incremental rotation vector at iteration $(i+1)$ is $\boldsymbol{\vartheta}_{n+1}^{(i)} + \Delta\boldsymbol{\vartheta}_{n+1}^{(i)}$, it follows from (81) and (86) that

$$\Delta\boldsymbol{\vartheta}_{n+1}^{(i)} \cdot \mathbf{e} = 0 \tag{89}$$

Similarly, we can conclude from (82) and (87) that

$$\Delta\boldsymbol{\theta}_{n+1}^{(i)} \cdot \mathbf{t}_n = 0, \quad \Delta\boldsymbol{\theta}_{n+1}^{(i)} \cdot \mathbf{t}_{n+1}^{(i+1)} = 0 \tag{90}$$

Relations (89) and $(90)_1$ are equivalent.

5 Implicit time integration schemes for constrained rotations

5.1 Description of the problem

In the computation dynamics, besides computation of displacements and rotations, one also needs to obtain velocities and accelerations at the chosen instant in the time interval of interest. We use the Newmark family of algorithms for that end; for energy conserving algorithms see e.g. [Simo and Tarnow (1994), Brank, Briseghella, Tonello and Damjanić (1998), Briseghella, Majorana and Pavan (2001)]. Standard implementation is used for computing the translational motion components, and necessary modifications are proposed for computing the components related to the constrained rotation of the shell-director.

Considering the typical time interval between t_n and t_{n+1} the algorithmic problem can be described as: Given at time t_n displacement, $\boldsymbol{\varphi}_n$, velocity, $\dot{\boldsymbol{\varphi}}_n$, and acceleration, $\ddot{\boldsymbol{\varphi}}_n$, of translational motion of the shell mid-surface, and shell-director, $\mathbf{t}_n$, its constrained rotation, $\boldsymbol{\Lambda}_n$, velocity, $\dot{\mathbf{t}}_n$, and acceleration, $\ddot{\mathbf{t}}_n$, find such values of $\boldsymbol{\varphi}$ and $\mathbf{t}$ at time t_{n+1} that

$$\delta\Pi_{dyn}\,|_{n+1} + \delta\Pi_{stat}\,|_{n+1} = 0 \tag{91}$$

and update velocities and accelerations of displacements and shell director by using the corresponding Newmark approximations. The update for displacements, constrained rotation tensors and shell-director vectors, which we need when solving (91) iteratively by Newton solution procedure, was discussed in the previous section. In this section, we address the remaining ingredients of the problem, namely the update of velocities and accelerations.

5.2 Newmark scheme for displacements

For a non-linear dynamics problem with translational degrees of freedom only, the standard implementation of the Newmark algorithm can be used. We compute the velocities and accelerations at time t_{n+1} with

$$\dot{\boldsymbol{\varphi}}_{n+1} = \frac{\gamma}{\beta h}\mathbf{u}_{n+1} + \frac{\beta-\gamma}{\beta}\dot{\boldsymbol{\varphi}}_n + \frac{(\beta-0.5\gamma)\,h}{\beta}\ddot{\boldsymbol{\varphi}}_n \tag{92}$$

$$\ddot{\boldsymbol{\varphi}}_{n+1} = \frac{1}{\beta h^2}\mathbf{u}_{n+1} - \frac{1}{\beta h}\dot{\boldsymbol{\varphi}}_n - \frac{0.5-\beta}{\beta}\ddot{\boldsymbol{\varphi}}_n \tag{93}$$

where β and γ are free Newmark parameters and $h = t_{n+1} - t_n$ is a typical time step. Typical choice for $\beta = 1/4$ and $\gamma = 1/2$ leads to the scheme of second-order accuracy.

5.3 Newmark scheme for constrained finite rotations; material form

It was noted in [Simo and Vu-Quoc (1988), Ibrahimbegović and Al Mikdad (1998) and Iura and Atluri (1988)] in their work on beams that Newmark approximations for angular velocity and acceleration can directly be applied only in the material representation as

$$\dot{\boldsymbol{\psi}}_{n+1} = \frac{\gamma}{\beta h}\boldsymbol{\vartheta}_{n+1} + \frac{\beta-\gamma}{\beta}\dot{\boldsymbol{\psi}}_n + \frac{(\beta-0.5\gamma)\,h}{\beta}\ddot{\boldsymbol{\psi}}_n \tag{94}$$

$$\ddot{\boldsymbol{\psi}}_{n+1} = \frac{1}{\beta h^2}\boldsymbol{\vartheta}_{n+1} - \frac{1}{\beta h}\dot{\boldsymbol{\psi}}_n - \frac{0.5-\beta}{\beta}\ddot{\boldsymbol{\psi}}_n \tag{95}$$

where $\boldsymbol{\vartheta}_{n+1}$ is material incremental rotation vector which is zero at t_n, while $\dot{\boldsymbol{\psi}}_n$ and $\ddot{\boldsymbol{\psi}}_n$ are material angular velocity and material angular acceleration at t_n. These approximations make sense geometrically also for shells, since all vectors in (94) and (95) are constrained by lying in the $\mathbb{R}^2$ plane perpendicular to the fixed base vector $\mathbf{e}$, see (81), (46) and (69), or, in another interpretation, in the plane tangential to the mid-surface at the reference configuration.

Shell-director velocity follows from (44)

$$\dot{\mathbf{t}}_{n+1} = \boldsymbol{\Lambda}_{n+1}\left(\dot{\boldsymbol{\psi}}_{n+1}\times\mathbf{e}\right) \tag{96}$$

and the shell-director acceleration from (64)

$$\ddot{\mathbf{t}}_{n+1} = \boldsymbol{\Lambda}_{n+1}\left(-\mathbf{e}\dot{\psi}^2_{n+1} + \ddot{\boldsymbol{\psi}}_{n+1}\times\mathbf{e}\right) \tag{97}$$

where $\boldsymbol{\Lambda}_{n+1} = \boldsymbol{\Lambda}_n\tilde{\boldsymbol{\Lambda}}\left(\boldsymbol{\vartheta}_{n+1}\right)$. By inserting equations (92), (93), (96) and (97) into the weak form of the balance equations, (91), we obtain a system of non-linear equations in incremental displacements $\mathbf{u}_{n+1}$ and incremental material rotation vector $\boldsymbol{\vartheta}_{n+1}$.

5.4 Newmark scheme for constrained finite rotations; spatial form

If we multiply expressions (94) and (95) from the left hand side by $\boldsymbol{\Lambda}_n$, and use material-spatial transformations for the rotational objects, we obtain

$$\boldsymbol{\Lambda}_n\dot{\boldsymbol{\psi}}_{n+1} = \frac{\gamma}{\beta h}\boldsymbol{\theta}_{n+1} + \frac{\beta-\gamma}{\beta}\dot{\mathbf{w}}_n + \frac{(\beta-0.5\gamma)\,h}{\beta}\ddot{\mathbf{w}}_n \tag{98}$$

$$\boldsymbol{\Lambda}_n\ddot{\boldsymbol{\psi}}_{n+1} = \frac{1}{\beta h^2}\boldsymbol{\theta}_{n+1} - \frac{1}{\beta h}\dot{\mathbf{w}}_n - \frac{0.5-\beta}{\beta}\ddot{\mathbf{w}}_n \tag{99}$$

If we further multiply the left hand side of (98) and (99) by identity $\tilde{\boldsymbol{\Lambda}}^T\left(\boldsymbol{\theta}_{n+1}\right)\tilde{\boldsymbol{\Lambda}}\left(\boldsymbol{\theta}_{n+1}\right)$, we end up with the spatial form of the Newmark approximations for finite rotations (see also [Ibrahimbegović and Al Mikdad (1998)])

$$\dot{\mathbf{w}}_{n+1} = \tilde{\boldsymbol{\Lambda}}\left(\boldsymbol{\theta}_{n+1}\right)\left[\frac{\gamma}{\beta h}\boldsymbol{\theta}_{n+1} + \frac{\beta-\gamma}{\beta}\dot{\mathbf{w}}_n + \frac{(\beta-0.5\gamma)\,h}{\beta}\ddot{\mathbf{w}}_n\right] \tag{100}$$

$$\ddot{\mathbf{w}}_{n+1} = \tilde{\boldsymbol{\Lambda}}\left(\boldsymbol{\theta}_{n+1}\right)\left[\frac{1}{\beta h^2}\boldsymbol{\theta}_{n+1} - \frac{1}{\beta h}\dot{\mathbf{w}}_n - \frac{0.5-\beta}{\beta}\ddot{\mathbf{w}}_n\right] \tag{101}$$

where $\boldsymbol{\theta}_{n+1}$, and $\dot{\mathbf{w}}$ and $\ddot{\mathbf{w}}$ at any time instant are constrained by (82), (47) and (70), respectively. However, as already mentioned in section 3.4, those constraints cannot be exploited to reduce the coordinate representation of the spatial form of angular velocity and acceleration.

Shell-director velocity at t_{n+1} follows from (45)

$$\dot{\mathbf{t}}_{n+1} = \dot{\mathbf{w}}_{n+1} \times \mathbf{t}_{n+1} \tag{102}$$

and acceleration of the shell-director vector follows from (65)

$$\ddot{\mathbf{t}}_{n+1} = \ddot{\mathbf{w}}_{n+1} \times \mathbf{t}_{n+1} - \mathbf{t}_{n+1}\dot{w}_{n+1}^2 \tag{103}$$

Their more elaborate forms are

$$\dot{\mathbf{t}}_{n+1} = \tilde{\mathbf{\Lambda}}\left(\boldsymbol{\theta}_{n+1}\right)\left[\frac{\gamma}{\beta h}\boldsymbol{\theta}_{n+1} \times \mathbf{t}_{n+1} + \frac{\beta-\gamma}{\beta}\dot{\mathbf{w}}_n \times \mathbf{t}_{n+1} + \frac{\left(\beta-0.5\gamma\right)h}{\beta}\ddot{\mathbf{w}}_n \times \mathbf{t}_{n+1}\right] \tag{104}$$

and

$$\begin{aligned}\ddot{\mathbf{t}}_{n+1} &= \tilde{\mathbf{\Lambda}}\left(\boldsymbol{\theta}_{n+1}\right)\left[\tfrac{1}{\beta h^2}\boldsymbol{\theta}_{n+1} \times \mathbf{t}_{n+1} - \tfrac{1}{\beta h}\dot{\mathbf{w}}_n \times \mathbf{t}_{n+1} - \tfrac{0.5-\beta}{\beta}\ddot{\mathbf{w}}_n \times \mathbf{t}_{n+1}\right] \\ &- \mathbf{t}_{n+1}\left[\tfrac{\gamma^2}{\beta^2 h^2}\boldsymbol{\theta}_{n+1}\cdot\boldsymbol{\theta}_{n+1} + \tfrac{(\beta-\gamma)^2}{\beta^2}\dot{\mathbf{w}}_n\cdot\dot{\mathbf{w}}_n + \tfrac{(\beta-0.5\gamma)^2}{\beta^2}h^2\ddot{\mathbf{w}}_n\cdot\ddot{\mathbf{w}}_n\right] \\ &- 2\mathbf{t}_{n+1}\left[\tfrac{(\beta-\gamma)\gamma}{\beta^2 h}\boldsymbol{\theta}_{n+1}\cdot\dot{\mathbf{w}}_n + \tfrac{(\beta-0.5\gamma)\gamma}{\beta^2}\boldsymbol{\theta}_{n+1}\cdot\ddot{\mathbf{w}}_n + \tfrac{(\beta-\gamma)(\beta-0.5\gamma)h}{\beta^2}\dot{\mathbf{w}}_n\cdot\ddot{\mathbf{w}}_n\right]\end{aligned} \tag{105}$$

The equivalence of (96) and (102) and of (97) and (103) follows immediately by using the transformation rules between the material and the spatial rotational objects.

When inserting equations (92), (93), (102) and (103) into the weak form of the balance equations, (91), we obtain a system of non-linear equations in incremental displacements $\mathbf{u}_{n+1}$ and incremental spatial rotation vector $\boldsymbol{\theta}_{n+1}$.

5.5 Newmark scheme in terms of the shell-director vector

Another possibility to obtain the shell-director velocity and acceleration at time t_{n+1} is to use Newmark approximations directly in terms of the shell-director vector time derivatives

$$\dot{\mathbf{t}}_{n+1} = \frac{\gamma}{\beta h}\left(\mathbf{t}_{n+1} - \mathbf{t}_n\right) + \frac{\beta-\gamma}{\beta}\dot{\mathbf{t}}_n + \frac{\beta-0.5\gamma}{\beta}h\ddot{\mathbf{t}}_n \tag{106}$$

$$\ddot{\mathbf{t}}_{n+1} = \frac{1}{\beta h^2}\left(\mathbf{t}_{n+1} - \mathbf{t}_n\right) - \frac{1}{\beta h}\dot{\mathbf{t}}_n - \frac{0.5-\beta}{\beta}\ddot{\mathbf{t}}_n \tag{107}$$

In order to compare this scheme with the one of the previous section, we insert (102) and (103) into (104) and (105), respectively. We get

$$\dot{\mathbf{t}}_{n+1} = \tilde{\mathbf{\Lambda}}\left(\boldsymbol{\theta}_{n+1}\right)\left[\frac{\gamma}{\beta h}\boldsymbol{\theta}_{n+1} \times \mathbf{t}_n + \frac{\beta-\gamma}{\beta}\dot{\mathbf{t}}_n + \frac{\left(\beta-0.5\gamma\right)h}{\beta}\left(\ddot{\mathbf{t}}_n + \mathbf{t}_n\dot{w}_n^2\right)\right] \tag{108}$$

$$\begin{aligned}\ddot{\mathbf{t}}_{n+1} &= \tilde{\mathbf{\Lambda}}\left(\boldsymbol{\theta}_{n+1}\right)\left[\tfrac{\gamma}{\beta h}\boldsymbol{\theta}_{n+1} \times \mathbf{t}_n - \tfrac{1}{\beta h}\dot{\mathbf{t}}_n - \tfrac{0.5-\beta}{\beta}\left(\ddot{\mathbf{t}}_n + \mathbf{t}_n\dot{w}_n^2\right)\right] \\ &- \mathbf{t}_{n+1}\left[\tfrac{\gamma^2}{\beta^2 h^2}\theta_{n+1}^2 + \tfrac{(\beta-\gamma)^2}{\beta^2}\dot{w}_n^2 + \tfrac{(\beta-0.5\gamma)^2h^2}{\beta^2}\ddot{w}_n^2\right] \\ &- 2\mathbf{t}_{n+1}\left[\tfrac{(\beta-\gamma)\gamma}{\beta^2 h}\boldsymbol{\theta}_{n+1}\cdot\dot{\mathbf{w}}_n + \tfrac{(\beta-0.5\gamma)\gamma}{\beta^2}\boldsymbol{\theta}_{n+1}\cdot\ddot{\mathbf{w}}_n + \tfrac{(\beta-\gamma)(\beta-0.5\gamma)h}{\beta^2}\dot{\mathbf{w}}_n\cdot\ddot{\mathbf{w}}_n\right]\end{aligned} \tag{109}$$

Some similarities may be noticed between expressions (106) and (108) as well as between (107) and (109); however further more detailed comparison is not obvious.

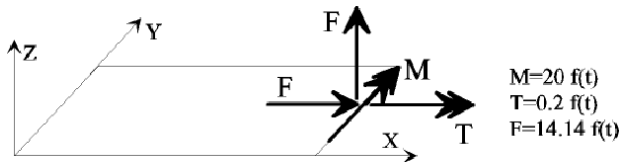

Figure 2: Beam-like plate: Geometry and loading data.

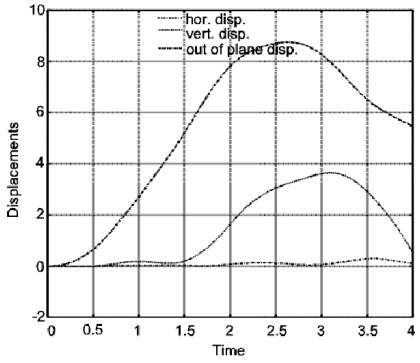

Figure 3: Beam-like plate: Displacement time histories for a point initially lying at (0,L,0).

6 Linearization aspects

6.1 Linearization of the shell-director motion

Let us recall that the dynamic part of the weak form of balance equations at time t_{n+1} is

$$\delta\Pi_{dyn,n+1} = \int_A \left[A_\rho \ddot{\boldsymbol{\varphi}}_{n+1} \cdot \delta\boldsymbol{\varphi} + I_\rho \ddot{\mathbf{t}}_{n+1} \cdot \delta\mathbf{t} \right] dA \tag{110}$$

where the test function $\delta\mathbf{t}$ has to satisfy the algorithmic form of (23)

$$\delta\mathbf{t} \cdot \mathbf{t}_{n+1} = 0 \tag{111}$$

By exploiting analogy with (50) and (51) we may write $\delta\mathbf{t}$ in terms of the incremental rotation vectors (introduced in section 4 and used for the time discretization in section 5) as

$$\begin{array}{rcl} \delta\mathbf{t} & = & \boldsymbol{\Lambda}_n \mathbf{A}^{\vartheta}_{n+1} \delta\boldsymbol{\vartheta} \\ \delta\mathbf{t} & = & \mathbf{A}^{\theta}_{n+1} \delta\boldsymbol{\theta} \end{array} \tag{112}$$

where $\mathbf{A}^{\vartheta}_{n+1}$ and $\mathbf{A}^{\theta}_{n+1}$, defined in (52) and (53), are now functions of the incremental rotation vectors $\boldsymbol{\vartheta}_{n+1}$ and $\boldsymbol{\theta}_{n+1}$, respectively. Eqs. (112) satisfy condition (111).

Linearization of $\delta\mathbf{t}$ with respect to intrinsic rotational variables at time t_{n+1}, which are $\boldsymbol{\vartheta}_{n+1}$ and $\boldsymbol{\theta}_{n+1}$, is not zero. It can be shown that the following forms can be obtained from (112)

$$\begin{array}{rcl} \Delta\delta\mathbf{t} \cdot \mathbf{b} & = & \delta\boldsymbol{\vartheta} \left[\tilde{\mathbf{Y}}^{\vartheta}_{n+1} \right] \Delta\boldsymbol{\vartheta}_{n+1} \\ \Delta\delta\mathbf{t} \cdot \mathbf{b} & = & \delta\boldsymbol{\theta} \left[\tilde{\mathbf{Y}}^{\theta}_{n+1} \right] \Delta\boldsymbol{\theta}_{n+1} \end{array} \tag{113}$$

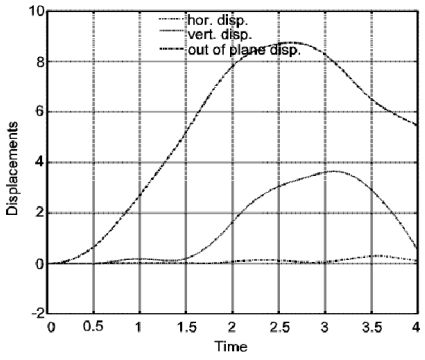

Figure 4: Beam-like plate: Velocity time histories for a point initially lying at (0,L,0).

where $\mathbf{b} \in \mathbb{R}^3$ and $\tilde{\mathbf{Y}}^{\vartheta}_{n+1}$ and $\tilde{\mathbf{Y}}^{\theta}_{n+1}$ are again functions of $\boldsymbol{\vartheta}_{n+1}$ and $\boldsymbol{\theta}_{n+1}$, respectively. Full form of $\tilde{\mathbf{Y}}^{\vartheta}_{n+1}$ is

$$\begin{array}{rcl} \tilde{\mathbf{Y}}^{\vartheta}_{n+1} & = & \frac{\vartheta\cos\vartheta-\sin\vartheta}{\vartheta^3}\left\{\boldsymbol{\vartheta}_{n+1}\otimes\boldsymbol{\vartheta}_{n+1}\left[(\boldsymbol{\Lambda}_n\mathbf{e})\cdot\mathbf{b}\right]+\mathbf{I}\left[(\boldsymbol{\Lambda}_n\left(\boldsymbol{\vartheta}_{n+1}\times\mathbf{e}\right))\cdot\mathbf{b}\right]\right\} \\ & - & \frac{\sin\vartheta}{\vartheta}\mathbf{I}\left[(\boldsymbol{\Lambda}_n\mathbf{e})\cdot\mathbf{b}\right] \\ & + & \frac{\sin\vartheta\left(3-\vartheta^2\right)-3\vartheta\cos\vartheta}{\vartheta^5}\left\{\boldsymbol{\vartheta}_{n+1}\otimes\boldsymbol{\vartheta}_{n+1}\left[(\boldsymbol{\Lambda}_n\left(\boldsymbol{\vartheta}_{n+1}\times\mathbf{e}\right))\cdot\mathbf{b}\right]\right\} \\ & + & \frac{\vartheta\cos\vartheta-\sin\vartheta}{\vartheta^3}\left\{\left[\mathbf{A}+\mathbf{A}^T\right]\left((\boldsymbol{\Lambda}_n\mathbf{e}_1)\cdot\mathbf{b}\right)+\left[\mathbf{B}+\mathbf{B}^T\right]\left((\boldsymbol{\Lambda}_n\mathbf{e}_2)\cdot\mathbf{b}\right)\right\} \end{array} \tag{114}$$

where $\vartheta = \|\boldsymbol{\vartheta}_{n+1}\|$ and matrices $\mathbf{A}$, $\mathbf{B}$ are defined as

$$\mathbf{A} = \begin{bmatrix} 0 & 0 \\ \vartheta^1_{n+1} & \vartheta^2_{n+1} \end{bmatrix}, \quad \mathbf{B} = \begin{bmatrix} -\vartheta^1_{n+1} & -\vartheta^2_{n+1} \\ 0 & 0 \end{bmatrix}, \quad \boldsymbol{\vartheta}_{n+1} = \left[\vartheta^1_{n+1}, \vartheta^2_{n+1}\right]^T \tag{115}$$

Full form of $\tilde{\mathbf{Y}}^{\theta}_{n+1}$ is given in an analogous way. Some further details may be found in [Brank, Perić and Damjanić (1997)].

Finally, we note that the linearization of the shell-director at time t_{n+1}, namely $\Delta\mathbf{t}_{n+1}$, may be expressed in terms of incremental rotational parameters as, see (112)

$$\begin{array}{rcl} \Delta\mathbf{t}_{n+1} & = & \boldsymbol{\Lambda}_n\mathbf{A}^{\vartheta}_{n+1}\Delta\boldsymbol{\vartheta}_{n+1} \\ \Delta\mathbf{t}_{n+1} & = & \mathbf{A}^{\theta}_{n+1}\Delta\boldsymbol{\theta}_{n+1} \end{array} \tag{116}$$

6.2 Linearization of the dynamic part of the weak form of balance equations

The linearization of $\delta\Pi_{dyn}$ at time t_{n+1} may be obtained by linearization of $\ddot{\boldsymbol{\varphi}}_{n+1}$ with respect to $\mathbf{u}_{n+1}$, by linearization of $\ddot{\mathbf{t}}_{n+1}$ with respect to intrinsic rotational variables at time t_{n+1}, and by exploiting one of the relations (113).

We can write linearized form of $\delta\Pi_{dyn}$ as

$$\Delta\delta\Pi_{dyn,n+1} = \int_A \left(A\,\rho\Delta\ddot{\boldsymbol{\varphi}}_{n+1}\cdot\delta\boldsymbol{\varphi} + I\,\rho\Delta\ddot{\mathbf{t}}_{n+1}\cdot\delta\mathbf{t} + I\,\rho\ddot{\mathbf{t}}_{n+1}\cdot\Delta\delta\mathbf{t}\right)dA \tag{117}$$

where linearization of the translational part is given trivially

$$\Delta\ddot{\boldsymbol{\varphi}}_{n+1} = \frac{d}{d\varepsilon}\,|_{\varepsilon=0}\,\left[\ddot{\boldsymbol{\varphi}}_{n+1}(\boldsymbol{\varphi}_n+\varepsilon\Delta\mathbf{u}_{n+1})\right] = \frac{1}{\beta h^2}\Delta\mathbf{u}_{n+1} \tag{118}$$

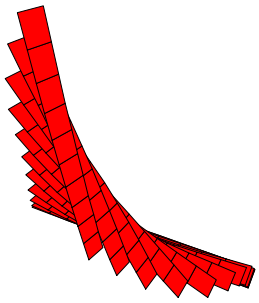

Figure 5: Beam-like plate: Deformed shapes; $0 \leq t \leq 2$ s (plot after every 0.2 s).

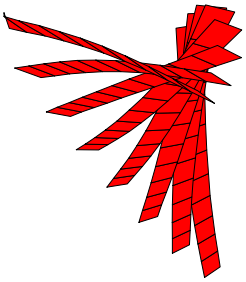

Figure 6: Beam-like plate: Deformed shapes; $2 \leq t \leq 3.6$ s (plot after every 0.2 s).

Expressions for $\Delta\delta\mathbf{t}$ are given in the previous section, while $\Delta\ddot{\mathbf{t}}_{n+1}$ is derived below.

Following (97) it may be written in terms of material axial velocity and acceleration as

$$\begin{aligned} \Delta\ddot{\mathbf{t}}_{n+1} &= \mathbf{\Lambda}_n \left[-\Delta\boldsymbol{\vartheta}_{n+1} \times \mathbf{e}\Delta\dot{\psi}^2_{n+1} + \Delta\boldsymbol{\vartheta}_{n+1} \times \left(\Delta\ddot{\boldsymbol{\psi}}_{n+1} \times \mathbf{e} \right) \right] \\ &+ \mathbf{\Lambda}_{n+1} \left[-2 \left(\mathbf{e} \otimes \dot{\boldsymbol{\psi}}_{n+1} \right) \Delta\dot{\boldsymbol{\psi}}_{n+1} + \Delta\ddot{\boldsymbol{\psi}}_{n+1} \times \mathbf{e} \right] \end{aligned} \tag{119}$$

where

$$\Delta\dot{\boldsymbol{\psi}}_{n+1} = \frac{\gamma}{\beta h}\Delta\boldsymbol{\vartheta}_{n+1}, \qquad \Delta\ddot{\boldsymbol{\psi}}_{n+1} = \frac{1}{\beta h^2}\Delta\boldsymbol{\vartheta}_{n+1} \tag{120}$$

We have expressed $\Delta\ddot{\mathbf{t}}_{n+1}$ with the linearized form of the material incremental rotation vector $\Delta\boldsymbol{\vartheta}_{n+1}$.

When working with spatial objects, we can exploit (103) to obtain

$$\begin{aligned} \Delta\ddot{\mathbf{t}}_{n+1} &= \Delta\ddot{\mathbf{w}}_{n+1} \times \mathbf{t}_{n+1} + \ddot{\mathbf{w}}_{n+1} \times \Delta\mathbf{t}_{n+1} - \Delta\mathbf{t}_{n+1}\dot{w}^2_{n+1} - \mathbf{t}_{n+1}2\dot{w}_{n+1}\Delta\dot{w}_{n+1} \\ &= \Delta\ddot{\mathbf{w}}_{n+1} \times \mathbf{t}_{n+1} + \ddot{\mathbf{w}}_{n+1} \times \Delta\mathbf{t}_{n+1} - \Delta\mathbf{t}_{n+1}\dot{w}^2_{n+1} - 2\left(\mathbf{t}_{n+1} \otimes \dot{\mathbf{w}}_{n+1}\right)\Delta\dot{\mathbf{w}}_{n+1} \end{aligned} \tag{121}$$

where

$$\Delta\dot{\mathbf{w}}_{n+1} = \frac{\gamma}{\beta h}\tilde{\mathbf{\Lambda}}\left(\boldsymbol{\theta}_{n+1}\right)\Delta\boldsymbol{\theta}_{n+1}, \qquad \Delta\ddot{\mathbf{w}}_{n+1} = \frac{1}{\beta h^2}\tilde{\mathbf{\Lambda}}\left(\boldsymbol{\theta}_{n+1}\right)\Delta\boldsymbol{\theta}_{n+1} \tag{122}$$

By exploiting relations $\Delta\boldsymbol{\theta}_{n+1} = \mathbf{\Lambda}_n\Delta\boldsymbol{\vartheta}_{n+1}$ and $\mathbf{\Lambda}_{n+1} = \tilde{\mathbf{\Lambda}}\left(\boldsymbol{\theta}_{n+1}\right)\mathbf{\Lambda}_n$, expressions (122) may be also given in terms of the incremental material rotation vector as

$$\Delta\dot{\mathbf{w}}_{n+1} = \frac{\gamma}{\beta h}\mathbf{\Lambda}_{n+1}\Delta\boldsymbol{\vartheta}_{n+1}, \qquad \Delta\ddot{\mathbf{w}}_{n+1} = \frac{1}{\beta h^2}\mathbf{\Lambda}_{n+1}\Delta\boldsymbol{\vartheta}_{n+1} \tag{123}$$

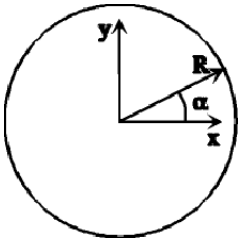

Figure 7: Short cylinder: geometry.

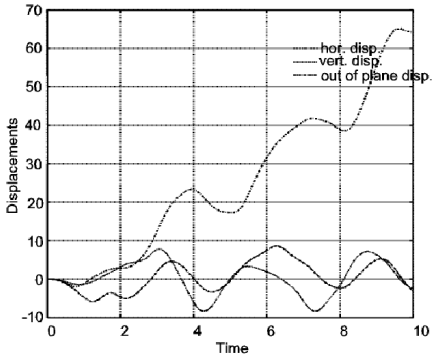

Figure 8: Short cylinder: Displacement time histories for a point initially lying at (0,-R,0).

We may therefore express $\Delta\ddot{\mathbf{t}}_{n+1}$ with $\Delta\boldsymbol{\theta}_{n+1}$ or $\Delta\boldsymbol{\vartheta}_{n+1}$. The equivalence of (119) and (121) can be shown by some simple manipulations.

7 Numerical simulations

7.1 Rotational parameters and procedures used

In this section we present results obtained in numerical simulations. All the computations are carried out by a research version of the computer program FEAP, developed by Prof. R. L. Taylor at UC Berkeley [Zienkiewicz and Taylor (1989)]. A four-noded isoparametric shell finite element with assumed strain interpolations for transverse strains (see e.g. [Brank, Perić and Damjanić (1995)] for details) is used to that end.

Table 2. Short cylinder: Loading data.

α	0	$\pi/2$	π	$3\pi/2$
Nodal loads	$[0,-1,-1]^T\,p(t)$	$[1,1,1]^T\,p(t)$	$[1,1,1]^T\,p(t)$	$[0,-1,-1]^T\,p(t)$

Time t	0.0	0.5	1.0
$p(t)$	0.0	5.0	0.0

Among the above discussed possible parametrizations of the shell-director motion, we have chosen the formulation based on the incremental material rotation vector. Note that within the

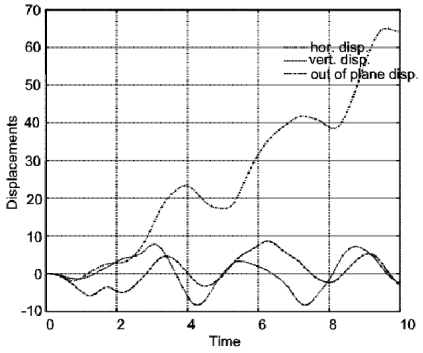

Figure 9: Short cylinder: Velocity time histories for a point initially lying at (0,-R,0).

interpolation presented in section 2.7, all possible parametrizations of constrained finite rotations should produce the same results, however they could differ in convergence characteristics and in the range of the allowable shell-director rotation where the solution can be obtained. Comparison of results for different rotation parameters for static loading may be found e.g. in [Betsch, Menzel and Stein (1998), Ibrahimbegović, Brank and Courtois (2001)].

Among the discussed Newmark time-stepping schemes for constrained finite rotations two different Newmark time-stepping schemes were coded. Algorithmic approximation of velocity and acceleration of the shell-director in time is obtained either with the spatial representation procedure described in section 5.4 (named 'version 1'), or with an alternative simpler procedure in terms of the shell-director vector, which is defined in section 5.5 (named 'version 2'). For both versions of Newmark time-stepping schemes the mass matrices are presented in the Appendix.

7.2 Example 1: Motion of a beam-like plate

The beam of length $L = 10$, width $B = 1$ and thickness $h = 0.5$ is initially lying in rest in the XY plane (see Figure 2). Its material characteristics are: Young's modulus $E = 21000$, Poisson's ratio $\nu = 0.2$ and mass density $\rho = 1$. Mid-surface mass density and inertia term with respect to the mid-surface are $A_\rho = h\rho = 0.5$ and $I_\rho = \frac{\rho h^3}{12} = 0.0104$, respectively. The beam is subjected to the external forces and moments which are applied at one end of the beam. Force vector is directed 45^0 from the mid-surface and has the following components with respect to X, Y, Z coordinate system: $\mathbf{f} = \{0, -14.14, 14.14\}^T$. Applied vector of moments is $\mathbf{m} = \{-20.00, 0.20, 0\}$, where its two non-zero components act in the direction of $-X$ and $+Y$ axis, respectively. The load is multiplied by a time function defined as: $f(t) = t$ for $t \in [0, 1]$; $f(t) = -t+2$ for $t \in [1, 2]$ and $f(t) = 0$ for $t > 2$.

The response of the beam is calculated up to 4 s with the time step $\Delta t = h = 0.01$ s. Displacements and velocities of the point A which at t_0 occupies position $(0, L, 0)$ are presented in Figures 3 and 4 where 'vertical', 'horizontal' and 'out of plane' denote the direction of X, Y and Z coordinate respectively. A sequence of deformed configurations during the initial 2 seconds (when the load is applied) is shown in Figure 5, while a sequence of deformed configurations between 2 and 3.6 seconds (when the beam is moving freely) is presented in Figure 6. The interval between two subsequent plotted configurations is 0.2 s.

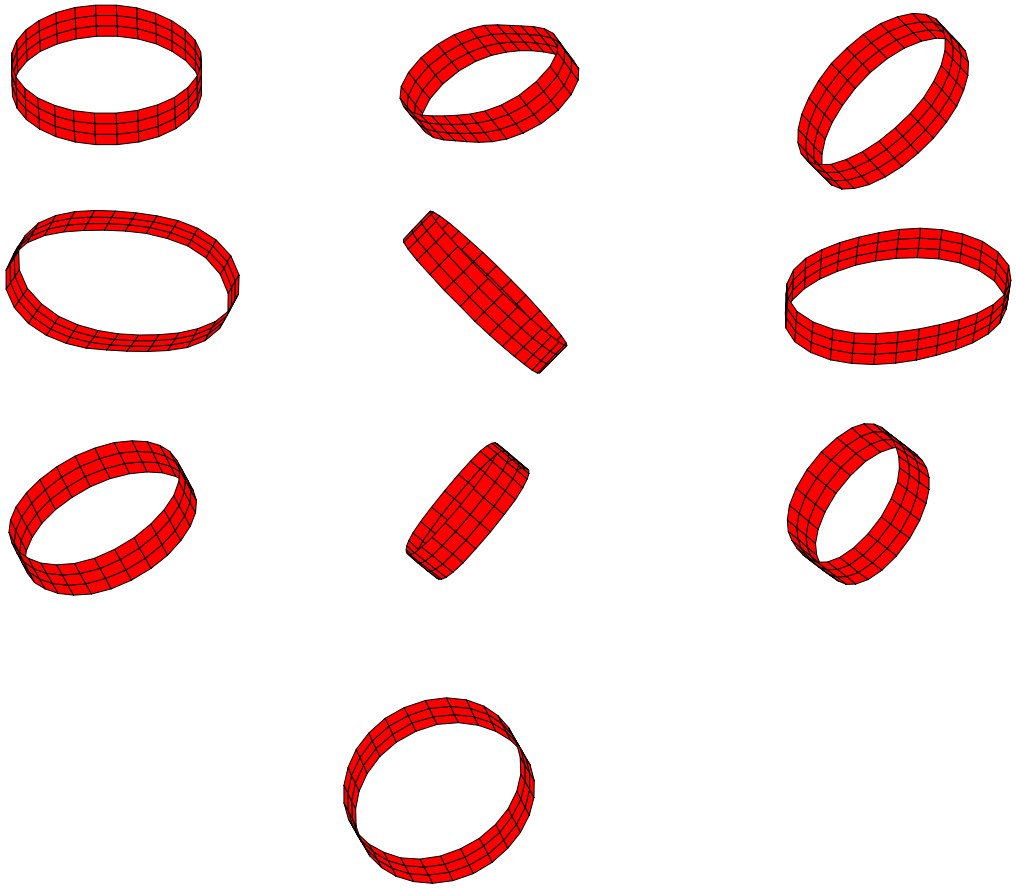

Figure 10: Short cylinder: Deformed configurations.

7.3 Example 2: Motion of a short cylinder

This example was considered by [Simo and Tarnow (1994) and Brank, Briseghella, Tonello and Damjanić (1998)]. Geometry of the short cylinder is defined by radius $R = 7.5$, height $H = 3$ and thickness $h = 0.02$. The material characteristics are: Young's modulus $E = 2 \times 10^8$, Poisson's ratio $\nu = 0.5$ and mass density $\rho = 1$. Mid-surface mass density and inertia term with respect to the mid-surface are $A_\rho = h\rho = 0.02$ and $I_\rho = \frac{\rho h^3}{12} = 6.667 \times 10^{-7}$, respectively. Loading conditions are presented in Figure 7 and Table 2. At time $t = 0$ the initial conditions are prescribed to be zero. The shell is subjected to impulsive loads acting from 0 until 1 second with the peak reached at 0.5 s. Response is calculated up to 10 s with the time step equal to $\Delta t = h = 0.05$ s. Evaluation of displacements and velocities of a point which is at $t = 0$ located at $(0, -R, 0)$ is presented in Figures 8 and 9, respectively. A sequence of deformed configurations is shown in Figure 10: at 0.25, 0.75, 1.25 s (first row); 1.75, 2.25, 2.75 s (second row); 3, 3.25, 3.5 s (third row) and 3.75 s.

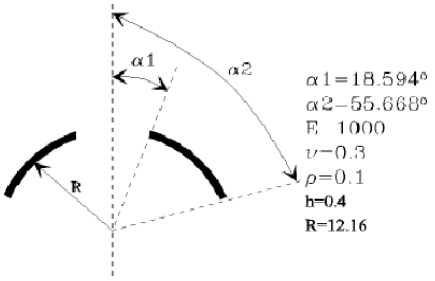

Figure 11: Spherical cup: Geometrical and material data.

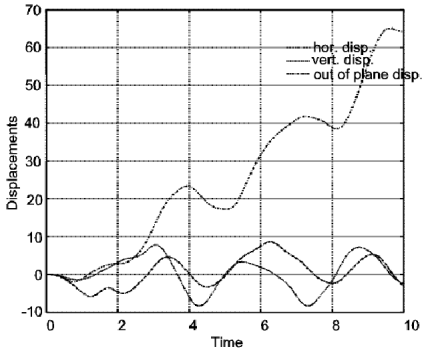

Figure 12: Spherical cup: Displacement time histories of the loaded ring.

7.4 Example 3: Dynamic snap-trough of a spherical cup

The geometry of the spherical cup and material characteristics are defined on Figure 11. At the bottom of the cap the displacements in the Z (i.e. vertical) direction are restricted to be zero. The mesh is composed of 32×8 finite elements. Force $f(t) = 1.5p\,(t)$, where $p(t) = t$ for $t \in [0, 1]$ and $p\,(t) = 1$ for $t > 1$, is applied at each of 32 nodes around the top hole in $-Z$ direction.

Table 3. Spherical cup. Convergence characteristics at $t = 0.12$ s.

	Version 1		Version 2	
Iter. No	Residual norm	Energy norm	Residual norm	Energy norm
1	1.78×10^{1}	3.97×10^{-1}	1.78×10^{1}	3.97×10^{-1}
2	1.20×10^{-2}	1.33×10^{-7}	1.20×10^{-2}	1.33×10^{-7}
3	2.95×10^{-8}	7.13×10^{-19}	2.95×10^{-8}	7.12×10^{-19}

Response is traced up to 3 s by using the time step $\Delta t = h = 0.01$ s. Two different time-integration schemes are used to calculate this example; the first one is described in section 5.4 and marked as 'version 1' in Figure 12, while the second one is described in section 5.5 and marked as 'version 2'. Figure 12 shows displacement in the $-Z$ direction of the nodes around the upper hole with respect to the time. It can be seen that the scheme which approximates the rotational objects themselves is much more stable that the scheme which interpolates the time derivatives of the shell-director. The divergence for 'version 2' occurs at approximately 4 s, while 'version 1' is perfectly stable up to 10 s. Up to the divergence of 'version 2', both schemes

give exactly the same results (see Table 3 for the convergence characteristics). In Figure 13 a sequence of deformed configurations is presented at 0.05, 0.7, 0.9 s (first row); 1.1, 1.3, 1.5 s (second row); 1.7, 1.9, 2.1 s (third row); 2.3, 2.5, 2.7 s (fourth row) and 2.9 s.

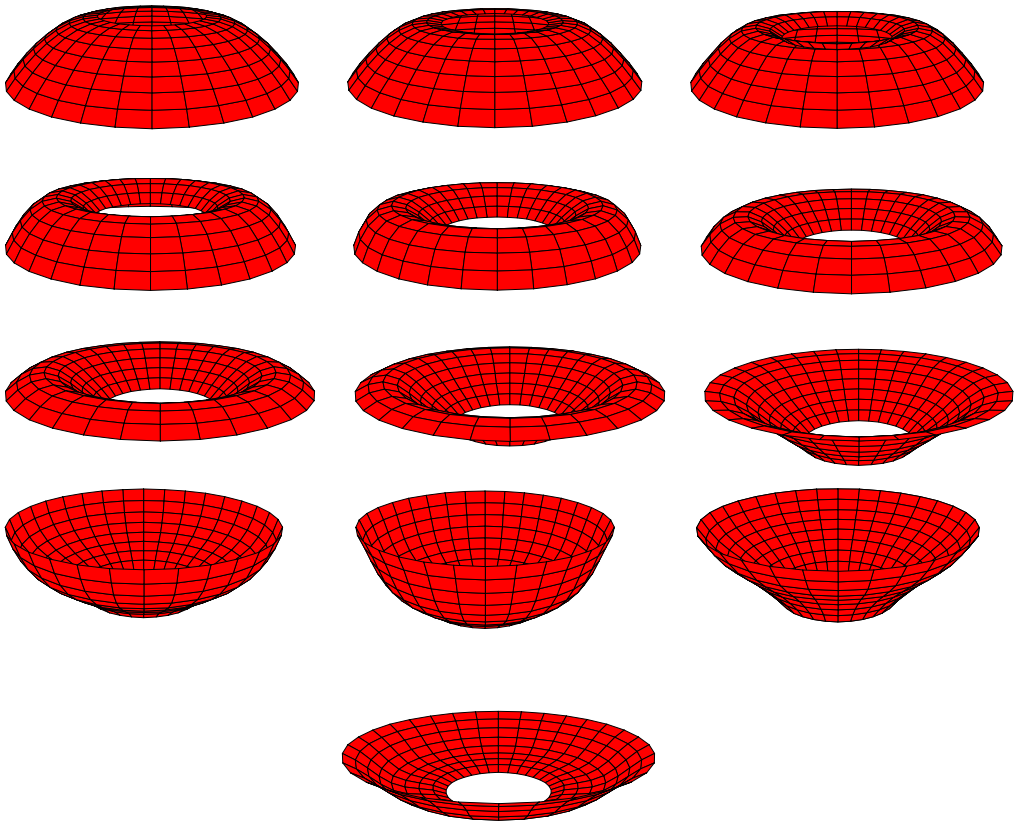

Figure 13: Spherical cup: Deformed configurations.

8 Conclusions

A detailed development of the parametrization of constrained finite rotations for dynamics of shells is presented. We recognized that the incremental rotation vector parameterization is the most suitable choice for handling the dynamics of shells in the sense of: (a) being able to avoid singularity problems, (b) maintaining simple additive iterative updates for rotations, and (c) being able to construct the 'displacement-like' Newmark schemes for rotational degrees of freedom.

Acknowledgements - This work was supported trough the Slovenia-France research collaboration PROTEUS and by the Ministry of Education, Science and Sport of Slovenia.

References

[1] Al Mikdad, M.; Ibrahimbegović, A. (1997): Dynamique et schémes d'intégration pour modèles de poutres géométricament exact. Revue europeenne des elements finis, 6, pp. 471-502.

[2] Başar Y.; Ding Y. (1990): Theory and finite element formulation for shell structures undergoing finite rotations. In Advances in the Theory of Plates and Shells (edited by G. Z. Voyiadjis and D. Karamanlidis), Elsevier, pp. 3-26.

[3] Başar Y.; Kintzel. O. (2001): Finite rotations and large strains in finite element shell analysis. CMES, 4, pp. 217-230.

[4] Betsch, P.; Menzel, A.; Stein, E. (1998): On the parametrization of finite rotations in computational mechanics. A classification of concepts with application to smooth shells. Comput. Methods Appl. Mech. Engrg., 155, 273-305.

[5] Brank, B.; Perić, D.; Damjanić, F.B. (1995): On implementation of a non-linear four-node shell finite element for thin multilayered elastic shells. Comp. Mech., 16, pp. 341-359.

[6] Brank, B.; Perić, D.; Damjanić, F.B. (1997): On large deformations of thin elasto-plastic shells: implementation of a finite rotation model for quadrilateral shell element. Int. J. Numer. Meth. Engng., 40, pp. 689-726.

[7] Brank, B.; Briseghella, L.; Tonello, N.; Damjanić, F.B. (1998): On non-linear dynamics of shells: Implementation of energy-momentum conserving algorithm for a finite rotation shell model. Int. J. Numer. Meth. Engng., 42, pp. 409-442.

[8] Brank, B.; Ibrahimbegović, A. (2001): On the relation between different parametrizations of finite rotations for shells. Eng. Comput., 18, pp. 950-973.

[9] Briseghella, L.; Majorana C.; Pavan P. (2001): A conservative time integration scheme for dynamics of elasto-damaged thin shells. CMES, 4, pp. 273-286.

[10] Büchter, N.; Ramm, E. (1992): Shell theory versus degeneration - a comparison in large rotation finite element analysis. Int. J. Numer. Meth. Engng., 34, pp. 39-59.

[11] Dvorkin, E.N.; Bathe, K.J. (1984): A continuum mechanics based four-node shell element for general nonlinear analysis. Eng. Comput., 1, pp. 77-84.

[12] Hughes, T. J. R. (1987): Finite Element Method: Linear Static and Dynamic Analysis, Prentice-Hall.

[13] Ibrahimbegović, A.; Frey, F; Kožar I. (1995): Computational aspects of vector-like parametrization of three-dimensional finite rotations. Int. J. Numer. Meth. Engng., 38, pp. 3653-3673.

[14] Ibrahimbegović, A. (1997): Stress resultant geometrically exact shell theory for finite rotations and it fe implementation. ASME Appl. Mech. Rewiev, 50, pp. 199-226.

[15] Ibrahimbegović, A. (1997a): On the choice of finite rotation parameters. Comp. Methods Appl. Mech. Eng., 149, pp. 49-71.

[16] Ibrahimbegović, A.; Al Mikdad, M. (1998): Finite rotations in dynamics of beams and implicit time-stepping schemes. Int. J. Numer. Meth. Engng., 41, pp. 781-814.

[17] Ibrahimbegović, A.; Brank, B.; Courtois, P. (2001): Stress resultant geometrically exact form of classical shell model and vector-like parametrization of constrained finite rotations. Int. J. Numer. Meth. Engng., 52, pp. 1235-1252.

[18] Ibrahimbegović, A.; Knopf-Lenoir C. (2001): Shape optimization of elastic structural systems undergoing large rotations: simultaneous solution procedure. CMES, 4, pp. 337-344.

[19] Iura M.; Atluri S.N. (1988): Dynamic analysis of finitely stretched and rotated three-dimensional space-curved beams. Computers and Structures, 29(5), pp. 875-889.

[20] Kegl M. (2000): Shape optimal design of structures: an efficient shape representation concept. Int. J. Numer. Meth. Engng., 49, pp. 1571-1588.

[21] Naghdi, P.M. (1972): The Theory of Shells and Plates. In Encyclopedia of Physics (edited by S. Flügge), Springer-Verlag.

[22] Simo J.C.; Hughes, T.J.R. (1986): On the variational foundations of assumed strain methods. J. Appl. Mech., 53, pp. 51-54.

[23] Simo, J.C.; Vu-Quoc, L. (1988): On the dynamics in space of rods undergoing large motions: a geometrically exact approach. Comp. Meth. Appl. Mech. Eng., 66, pp. 125-161.

[24] Simo, J.C.; Fox, D.D. (1989): On a stress resultant geometrically exact shell model, Part I: Formulation and optimal parametrization. Comp. Methods Appl. Mech. Eng., 72, pp. 267-304.

[25] Simo, J.C.; Fox, D.D.; Rifai, M.S. (1990): On a stress resultant geometrically exact shell model, Part III: The computational aspects of the nonlinear theory. Comp. Methods Appl. Mech. Eng., 79, pp. 21-70.

[26] Simo, J.C.; Rifai, M.S.; Fox, D.D. (1992): On stress resultant geometrically exact shell model. Part VI. Conserving algorithms for non-linear dynamics. Int. J. Numer. Meth. Engng., 34, pp. 117-164.

[27] Simo, J.C.; Tarnow, N. (1994): A new energy and momentum conserving algorithm for the nonlinear dynamics of shells. Int. J. Numer. Meth. Engng., 37, pp. 2527-2549.

[28] Suetake Y.; Iura M; Atluri S.N. (2001): Variational formulation and symmetric tangent operator for shells with finite rotation field. CMES, 4, pp. 329-336.

[29] Zienkiewicz, O.C.; Taylor, R.L. (1989): The Finite Element Method: Basic Formulation and Linear Problem. McGraw-Hill.

[30] Zupan, D.; Saje, M. (2001): A new finite element formulation of three-dimensional beam theory based on interpolation of curvature. CMES, 4, 301-318.

9 Appendix: Mass matrix

Mass matrix follows from the linearization of the dynamic part of the weak form of balance equations (117).

9.1 Incremental material rotation vector and spatial Newmark scheme for rotations

Let us first derive mass matrix for 'version 1' of time-interpolation of constrained rotations. By using equation (121) for $\Delta\ddot{\mathbf{t}}_{n+1}$, and expressing $\Delta\dot{\mathbf{w}}_{n+1}$ and $\Delta\ddot{\mathbf{w}}_{n+1}$ with relations (123), we get

$$\Delta\ddot{\mathbf{t}}_{n+1} = \left[\left(\frac{-1}{\beta h^2}\mathbf{T}_{n+1} - \frac{2\gamma}{\beta h}\left[\mathbf{t}_{n+1}\otimes\dot{\mathbf{w}}_{n+1}\right]\right)\mathbf{\Lambda}_{n+1} + \left(\ddot{\mathbf{W}}_{n+1} - \dot{w}^2_{n+1}\mathbf{I}\right)\mathbf{\Lambda}_n\mathbf{A}^{\vartheta}_{n+1}\right]\Delta\boldsymbol{\vartheta}_{n+1} \tag{124}$$

where $\mathbf{T}_{n+1}$ and $\ddot{\mathbf{W}}_{n+1}$ are skew-symmetric matrices, i.e. $\mathbf{T}_{n+1} = \mathbf{t}_{n+1}\times\mathbf{b}$ and $\ddot{\mathbf{W}}_{n+1} = \ddot{\mathbf{w}}_{n+1}\times\mathbf{b}$, $\mathbf{b}\in\mathbb{R}^3$. By defining variation, $\delta\mathbf{t}$, and linearization of variation, $\Delta\delta\mathbf{t}$, of the shell-director vector in terms of incremental material rotation vector, see (112) and (113), and by using continuum-consistent interpolations of section 2.7, we get the sub-matrix $\mathbf{M}_{IJ}$ of the finite element mass matrix of the following form

$$\mathbf{M}_{IJ} = \begin{bmatrix} N^I N^J \frac{A_\rho}{\beta h^2}\mathbf{I} & \mathbf{0}_{3\times 2} \\ \mathbf{0}_{2\times 3} & \begin{array}{l} N^I N^J I_\rho \left[\mathbf{A}^{\vartheta,I}_{n+1}\right]^T \left[\mathbf{\Lambda}^I_n\right]^T \times \\ \left[\left(\frac{-1}{\beta h^2}\mathbf{T}^J_{n+1} - \frac{2\gamma}{\beta h}\mathbf{t}^J_{n+1}\otimes\dot{\mathbf{w}}^J_{n+1}\right)\mathbf{\Lambda}^J_{n+1} + \right. \\ \left.\left(\ddot{\mathbf{W}}^J_{n+1} - \left(\dot{w}^J_{n+1}\right)^2\mathbf{I}\right)\mathbf{\Lambda}^J_n\mathbf{A}^{\vartheta,J}_{n+1}\right] + \\ N^I\tilde{\mathbf{Y}}^I I_\rho\delta^J_I \end{array} \end{bmatrix} \tag{125}$$

where $\mathbf{I}$ is a (3×3) unit matrix, $\mathbf{A}^{\vartheta,J}_{n+1}$ is a (3×2) matrix, δ^J_I is Kronecker delta and $\tilde{\mathbf{Y}}^I$ is a (2×2) matrix defined as (see (114))

$$\begin{aligned} \tilde{\mathbf{Y}}^I &= \tfrac{\vartheta\cos\vartheta-\sin\vartheta}{\vartheta^3}\left(-\begin{bmatrix} \left(\vartheta^{1,I}_{n+1}\right)^2 & \vartheta^{1,I}_{n+1}\vartheta^{2,I}_{n+1} \\ \vartheta^{1,I}_{n+1}\vartheta^{2,I}_{n+1} & \left(\vartheta^{2,I}_{n+1}\right)^2 \end{bmatrix}\left[\mathbf{t}^I_n\right]^T\ddot{\mathbf{t}}^I_{n+1} + \right. \\ &\qquad \left.\begin{bmatrix} 1 & 0 \\ 0 & 1 \end{bmatrix}\mathbf{\Lambda}^I_n\left\{\vartheta^{2,I}_{n+1}, -\vartheta^{1,I}_{n+1}, 0\right\}^T\ddot{\mathbf{t}}^I_{n+1}\right) \\ &- \tfrac{\sin\vartheta}{\vartheta}\begin{bmatrix} 1 & 0 \\ 0 & 1 \end{bmatrix}\left[\mathbf{t}^I_n\right]^T\ddot{\mathbf{t}}^I_{n+1} \\ &+ \tfrac{\sin\vartheta\left(3-\vartheta^2\right)-3\vartheta\cos\vartheta}{\vartheta^5}\begin{bmatrix} \left(\vartheta^{1,I}_{n+1}\right)^2 & \vartheta^{1,I}_{n+1}\vartheta^{2,I}_{n+1} \\ \vartheta^{1,I}_{n+1}\vartheta^{2,I}_{n+1} & \left(\vartheta^{2,I}_{n+1}\right)^2 \end{bmatrix}\mathbf{\Lambda}^I_n\left\{\vartheta^{2,I}_{n+1}, -\vartheta^{1,I}_{n+1}, 0\right\}^T\ddot{\mathbf{t}}^I_{n+1} \\ &+ \tfrac{\vartheta\cos\vartheta-\sin\vartheta}{\vartheta^3}\left(\begin{bmatrix} 0 & \vartheta^{1,I}_{n+1} \\ \vartheta^{1,I}_{n+1} & 2\left(\vartheta^{2,I}_{n+1}\right)^2 \end{bmatrix}\mathbf{\Lambda}^I_n\left\{1,0,0\right\}^T\ddot{\mathbf{t}}^I_{n+1} - \right. \\ &\qquad \left.\begin{bmatrix} 2\left(\vartheta^{1,I}_{n+1}\right)^2 & \vartheta^{2,I}_{n+1} \\ \vartheta^{2,I}_{n+1} & 0 \end{bmatrix}\mathbf{\Lambda}^I_n\left\{0,1,0\right\}^T\ddot{\mathbf{t}}^I_{n+1}\right) \end{aligned} \tag{126}$$

where $\vartheta = \left\|\boldsymbol{\vartheta}^I_{n+1}\right\|$, and $\vartheta^{1,I}_{n+1}$ and $\vartheta^{2,I}_{n+1}$ are two non-zero components of $\boldsymbol{\vartheta}^I_{n+1} = \left\{\vartheta^{1,I}_{n+1}, \vartheta^{2,I}_{n+1}\right\}^T$.

9.2 Incremental material rotation vector and Newmark scheme in terms of shell-director

For 'version 2' of time-interpolation of the shell-director motion we exploit expression (107). By its linearization with respect to the shell-director at time t_{n+1}, we obtain simple expression for

$\Delta\ddot{\mathbf{t}}_{n+1}$, namely $\Delta\ddot{\mathbf{t}}_{n+1} = \frac{1}{\beta h^2}\Delta\mathbf{t}_{n+1}$, which can be further elaborated by using (116) to get

$$\Delta\ddot{\mathbf{t}}_{n+1} = \frac{1}{\beta h^2}\mathbf{\Lambda}_n\mathbf{A}^{\vartheta}_{n+1}\Delta\boldsymbol{\vartheta}_{n+1} \tag{127}$$

Expressing variation, $\delta\mathbf{t}$, and linearization of variation, $\Delta\delta\mathbf{t}$, of the shell-director vector with (112) and (113), respectively, and by using continuum-consistent interpolations of section 2.7, we get the following form of the sub-matrix of mass matrix

$$\mathbf{M}_{IJ} = \begin{bmatrix} N^I N^J \frac{A_\rho}{\beta h^2}\mathbf{I} & \mathbf{0}_{3\times 2} \\ \mathbf{0}_{2\times 3} & \frac{1}{\beta h^2}N^I N^J I_\rho \left[\mathbf{A}^{\vartheta,I}_{n+1}\right]^T \left[\mathbf{\Lambda}^I_n\right]^T \mathbf{\Lambda}^J_n \mathbf{A}^{\vartheta,J}_{n+1} + \\ & N^I \tilde{\mathbf{Y}}^I I_\rho \delta^J_I \end{bmatrix} \tag{128}$$

which is of simpler form that the one presented in (125) for 'version 1'.